



- (51) International Patent Classification:  
*F03C 4/00* (2006.01)
- (21) International Application Number:  
PCT/US2012/023694
- (22) International Filing Date:  
2 February 2012 (02.02.2012)
- (25) Filing Language: English
- (26) Publication Language: English
- (30) Priority Data:  
61/438,951 2 February 2011 (02.02.2011) US
- (71) Applicant (for all designated States except US):  
**COLUMBIA POWER TECHNOLOGIES, INC.** [US/US]; 236 East High Street, Charlottesville, VA 22902 (US).
- (72) Inventors; and  
(75) Inventors/Applicants (for US only): **RHINEFRANK, Kenneth, Edward** [US/US]; 7740 NW Hoodview Circle, Corvallis, OR 97330 (US). **SCHACHER, Alphonse, Aloysius** [US/US]; 2872 SE Park Place, Corvallis, OR 97333 (US). **PRUDELL, Joseph, Horan** [US/US]; 3060 NW Garfield Ave, Corvallis, OR 97330 (US). **HAM-MAGREN, Erik, Joel** [US/US]; 690 SE Bayshore Circle, Corvallis, OR 97333 (US).
- (74) Agent: **FARRELL, Kevin, M.**; Pierce Atwood LLP, 100 Summer Street, Suite 2250, Boston, MA 02110 (US).
- (81) Designated States (unless otherwise indicated, for every kind of national protection available): AE, AG, AL, AM, AO, AT, AU, AZ, BA, BB, BG, BH, BR, BW, BY, BZ, CA, CH, CL, CN, CO, CR, CU, CZ, DE, DK, DM, DO, DZ, EC, EE, EG, ES, FI, GB, GD, GE, GH, GM, GT, HN, HR, HU, ID, IL, IN, IS, JP, KE, KG, KM, KN, KP, KR, KZ, LA, LC, LK, LR, LS, LT, LU, LY, MA, MD, ME, MG, MK, MN, MW, MX, MY, MZ, NA, NG, NI, NO, NZ, OM, PE, PG, PH, PL, PT, QA, RO, RS, RU, RW, SC, SD, SE, SG, SK, SL, SM, ST, SV, SY, TH, TJ, TM, TN, TR, TT, TZ, UA, UG, US, UZ, VC, VN, ZA, ZM, ZW.
- (84) Designated States (unless otherwise indicated, for every kind of regional protection available): ARIPO (BW, GH, GM, KE, LR, LS, MW, MZ, NA, RW, SD, SL, SZ, TZ, UG, ZM, ZW), Eurasian (AM, AZ, BY, KG, KZ, MD, RU, TJ, TM), European (AL, AT, BE, BG, CH, CY, CZ, DE, DK, EE, ES, FI, FR, GB, GR, HR, HU, IE, IS, IT, LT, LU, LV, MC, MK, MT, NL, NO, PL, PT, RO, RS, SE, SI, SK, SM, TR), OAPI (BF, BJ, CF, CG, CI, CM, GA, GN, GQ, GW, ML, MR, NE, SN, TD, TG).
- Published:  
— without international search report and to be republished upon receipt of that report (Rule 48.2(g))

(54) Title: METHOD AND SYSTEM FOR WAVE ENERGY CONVERSION

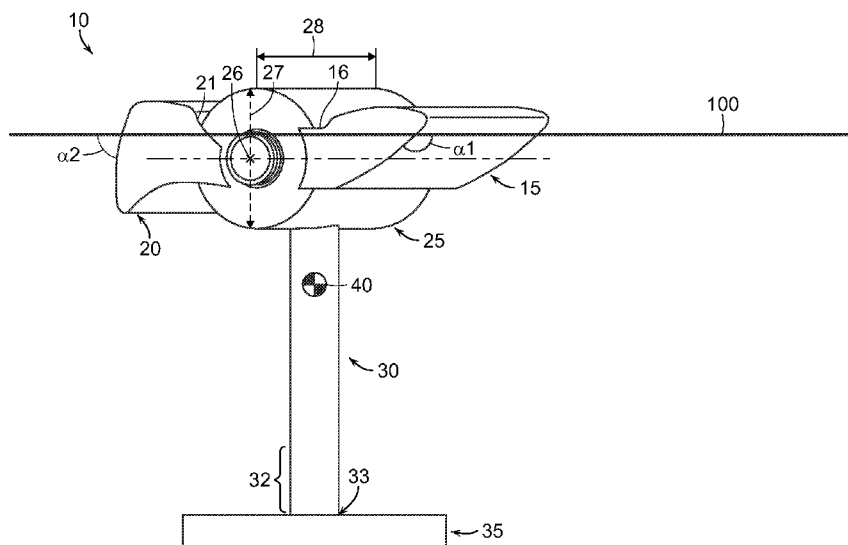


FIG. 1

(57) Abstract: An apparatus and method for converting wave energy using the relative rotational movement between two interconnected float assemblies and the relative rotational movement between each of the float assemblies and a spar which extends from a connection with the float assemblies at the water surface into the water.

## METHOD AND SYSTEM FOR WAVE ENERGY CONVERSION

## CROSS REFERENCE TO RELATED APPLICATION

[0001] The present application is related to and claims the benefit of priority to U.S. provisional patent application No. 61/438,951 filed on Feb. 2, 2010, the entire contents of which are incorporated herein by reference.

## BACKGROUND

## 1. Field of the Invention

[0002] The present invention relates generally to converting wave surge and heave into energy and more particularly to optimizing hydrodynamic bodies for maximum energy production for wave energy conversion (WEC).

## 2. Discussion of Background information

[0003] Because ocean waves exist everywhere in the world and behave predictably in distinct regions, converting the energy in these waves to electricity could provide a predictable, reliable supply of electricity to electric power systems in many parts of the world. Approximately seventy percent (70%) of the population of the entire world lives within two hundred miles of an ocean, making that an accessible source of renewable energy. Water waves that form in large bodies of water contain kinetic and potential energy that the device and methodology of the present invention is designed to extract. Existing wave energy conversion devices typically capture surge or heave and fail to capture fully the rotational energy of a wave. Conventional shapes and designs of articulating wave energy buoys are typically simple floating structures such as a raft or a tube and typically lack effective energy capture for producing an energy to cost ratio.

[0004] A need therefore exists for a wave energy conversion apparatus that efficiently converts the hydrodynamic surge (horizontal component) and heave (vertical component) of

rotational ocean wave energy into rotary shaft motion for use in direct drive rotary generation.

## SUMMARY OF THE INVENTION

[0005] One embodiment of the wave energy converter includes a first rotational float having a first angle of attack relative to the horizon and a second rotational float having a second angle of attack relative to the horizon; a sealed nacelle enclosure having a central longitudinal axis at both ends of which are disposed power take offs, a first power take off being mechanically coupled to the first rotational float and a second power take off being mechanically coupled to the second rotational float, and a spar having a top end mated with the nacelle and a bottom end mated with a heave plate. In one embodiment, the spar and damper extend into a body of water while the first rotational float and said second rotational float are supported at the water surface such that wave heave and wave surge forces rotate the first rotational float in opposite directions to the mated nacelle and spar and the second float rotates in opposite directions to the mated nacelle and spar. .

[0006] In another aspect, the present invention provides a method for generating power. In one embodiment the method includes providing a first rotational float having a first angle of attack relative to the horizon and a second rotational float having a second angle of attack relative to the horizon, and providing a sealed nacelle enclosure having a central longitudinal axis at both ends of which are disposed power take offs, a first power take off being mechanically coupled to the first rotational float and a second power take off being mechanically coupled to the second rotational float. The method includes providing a spar having a top end mated with the nacelle and a bottom end mated with a heave plate, wherein the spar and damper extend into a body of water while the first rotational float and said second rotational float are supported at the water surface such that wave heave and wave surge forces rotate the first rotational float in opposite directions to the mated nacelle and spar and the second float rotates in opposite directions to the mated nacelle and spar. The method includes assembling a wave energy converter unit by attaching the first rotational float and second rotational float to the nacelle and attaching the nacelle to the spar, and deploying the wave energy converter within a wave field.

## BRIEF DESCRIPTION OF THE DRAWINGS

[0007] One will better understand these and other features, aspects, and advantages of the present invention following a review of the description, appended claims, and accompanying drawings in which:

[0008] FIG. 1 is an isometric view of an illustrative embodiment of a wave energy converter;

[0009] FIG. 2 is side view of the illustrative embodiment of FIG. 1;

[0010] FIG. 3 is perspective partial view of portions of the illustrative embodiment of FIG. 1;

[0011] FIGS. 4 is a perspective view of a portion of the illustrative embodiment of FIG. 1;

[0012] FIG. 5 is a perspective view of the portion of FIG. 4;

[0013] FIG. 6 is a perspective view of a portion of the illustrative embodiment of FIG. 1;

[0014] FIG. 7 is a perspective view of the portion of FIG. 6;

[0015] FIG. 8 is perspective view of portions of FIG. 3;

[0016] FIG. 9 is schematic side view of an illustrative embodiment of the wave energy converter;

[0017] FIG. 10 is an isometric view of an embodiment of a wave energy converter;

[0018] FIG. 11 is a partial view of FIG. 10.

[0019] FIG. 12 is a partial view of FIG. 10 showing a second plate utilized to optimize

spar body motion if parallel to the wave front or to act as a keel if perpendicular to the incoming waves.

[0020] FIG. 13 depicts the original Manta\_001 prior art shape versus a performance optimized Manta\_344 shape of the present invention according to the 344<sup>th</sup> shape investigation.

[0021] FIG. 14; is a description of body motions in all six degrees of freedom: surge, sway, heave, roll, pitch, yaw.

[0022] FIG. 15; Phase relationship between forward float and spar. Phase relationship between aft float and spar.

[0023] FIG. 16; Average power production versus maximum design power take off torque.

[0024] FIG. 17; Response amplitude operator (RAO) for forward & aft float torque with torque limited at  $4.106 \times 10^6$  Nm.

[0025] FIG. 18 is Power flux of sample wave energy spectrum

[0026] FIG. 19 is a gradient map of best case damping as a function of peak energy period ( $T_p$ ) and significant wave height ( $H_s$ ).

[0027] FIG. 20 is a gradient map of energy produced as a function of peak energy period ( $T_p$ ) and significant wave height ( $H_s$ ) with annual occurrence reported in hours for each occurrence ( $H_{mo}-T_p$ ).

[0028] FIG. 21 is a table of mass inertia, center of gravity, total volume for each body (spar, forward float, aft float).

[0029] FIG. 22 is a relative capture width (RCW) vs. wave period plot.

[0030] FIG. 23 is representative plots of Active RAO's and phase relationships for all

bodies studied. C1=Case 1, C2= case 2, etc.

[0031] FIG. 24 is representative plots of Active RAO's and phase relationships for all bodies studied. C1=Case 1, C2= case 2, etc

[0032] FIG. 25 is a plot of damping applied at PTO versus wave period.

[0033] FIG. 26 is a plot of energy available in the wave climate (Raw) and energy absorbed by the WEC (OR, HUM).

[0034] FIG. 27 is a bar graph of Max energy (Max) in wave climate, energy delivered by the WEC (WEC) and energy delivered using nameplate calculation (NP).

[0035] FIG. 28 is a bar graph of Max energy (Max) in wave climate, energy delivered by the WEC (WEC) and energy delivered using nameplate calculation (NP).

[0036] FIG. 29 is a bar graph of nameplate energy calculation for Oregon and Humboldt.

[0037] FIG. 30 is gradient map of RCW as a function of  $T_p$  (peak energy period) and  $T$  (wave period) for case 1.

[0038] FIG. 31 is gradient map of RCW as a function of  $T_p$  and  $T$  for case 2.

[0039] FIG. 32 is an illustrative analysis of one case of an active RCW from PM spectrum shown in a 3D view for one embodiment of the WEC.

[0040] FIG.33 is an illustrative analysis of one case of an active RCW from PM spectrum shown in a 3D view for one embodiment of the WEC.

[0041] FIG. 34 is an illustrative analysis of an active RAO's and phase from PM spectrum for two embodiments of the WEC.

[0042] FIG. 35 is an illustrative analysis of damping conditions from PM spectrum for two embodiments of the WEC

[0043] FIG. 36 is an illustrative analysis of one case of damping selection for one embodiment of the WEC.

[0044] FIG. 37 is an illustrative analysis of one case of damping selection for one embodiment of the WEC.

[0045] FIG. 38 is an illustrative analysis of raw available energy from PM spectrum in two geographic locations and energy absorbed by the WEC for two embodiments of the WEC.

[0046] FIG. 39 is an illustrative analysis of energy climates from PM spectrum and energy absorbed by the WEC for one embodiment of the WEC deployed in one geographic region.

[0047] FIG. 40 is an illustrative analysis of energy climates from PM spectrum and energy absorbed by the WEC for one embodiment of the WEC deployed in one geographic region.

[0048] FIG. 41 is an illustrative analysis of active RCW from PM spectrum for two embodiments of the WEC.

## DETAILED DESCRIPTION

[0049] Several exemplary considerations differentiate embodiments of this wave converter from other wave converters. For example, in one implementation, maximization of relative motion between a forward float and a nacelle is accomplished by a design that maximizes heave and surge force on the forward float, while the nacelle is also optimized to maximize heave and surge forces on the nacelle. These features are optimized by properly selecting the shape, center of gravity, center of buoyancy, moment of inertia, freeboard and draft through empirical numerical analysis. As another example, maximization of relative motion between an aft float and the nacelle is accomplished by a design that maximizes heave and surge force on the aft float, while the nacelle is also optimized to maximize heave and surge forces on the nacelle. As with the forward float, these features are optimized by properly selecting the shape, center of gravity, moment of inertia, freeboard and draft through empirical numerical analysis.

[0050] Turning now to FIG. 1, a wave energy converter (hereinafter “WEC”) 10 includes a rotatable fore float 15 (also referred to as a “rotational first float”) having a first angle of attack  $\alpha_1$  relative to the horizon (here, the water surface) 100 and a rotatable aft float 20 (also referred to as a “rotational second float”) having a second angle of attack  $\alpha_2$  relative to the horizon. The rotatable fore float 15 and rotatable aft float 20 are attached to a nacelle 25 for rotation about a central longitudinal axis 26 of the nacelle 25. In the embodiment of FIG. 1, the WEC also includes a spar 30 having a top end mated with the nacelle 25 and a bottom end mated with at least one damper 35, or heave plate. In one embodiment, the spar 30 and at least one damper 35 extend into a body of water while the rotatable fore float 15 and rotatable aft float 20 are supported at the water surface 100 such that wave heave and wave surge forces rotate the rotatable fore float 15 in opposite directions to the mated nacelle 25 and spar 30 and the rotatable aft float 20 rotates in opposite directions to the mated nacelle 25 and spar 30.

[0051] Fluid waves are comprised of rotational particle motions which impart vertical up force and vertical down force on bodies exposed to the wave, and surge which imparts a horizontal force. The magnitude of the rotational force is highest at the surface of the water, diminishing as the water depth increases. The rotatable fore float 15 and rotatable aft float 20 have different angles of attack  $\alpha_1$ ,  $\alpha_2$  relative to the horizon so as to capture the rotational and

linear forces imparted by a wave. The wave motion rotates the rotatable fore float 15, rotatable aft float 20 and the nacelle 25 such that they transmit torque to a plurality of generators (not shown) enclosed within the nacelle 25.

[0052] FIGS. 3 through 8 depict one embodiment of the rotatable fore float 15 and rotatable aft float 20 in more detail. FIG. 3 depicts the rotatable fore float 15 and rotatable aft float 20 relative to the nacelle with a fore arm 16 and aft arm 21 removed. FIG. 4 depicts one embodiment of the fore float 15, which faces forward toward an oncoming wave. The fore float 15 comprises a fore arm 16a, the length of which is selected for optimum power extraction in a target wave climate. FIG. 5 depicts the fore float 15 with no fore arm 16a formed thereon or otherwise attached thereto. The top side 17 of the rotatable fore float 15 is designed to minimize materials (i.e. reduce costs) used to enclose the structure. For example; completing the structure with a semicircle requires more material and increases cost. All sides (e.g. top side 17, front side 18 and left side 19) of fore float 15 are slightly convex rather than flat. This slight curvature is designed to allow for composite manufacture on a wound mandrel. The curvature also allows for composite manufacture processes that use a mold. The front side 18 is optimized in both radius and slope in order to maximize energy capture from the incident wave climate. Hydrodynamic numerical analysis and optimization techniques were employed to design the float to maximize power delivered from the rotatable fore float 15 while minimizing the material utilized. Thus this shape (slope and radius) is the result of an optimized power to cost ratio. In a plan view perspective, the front side 18 of the fore float 15 is rectangularly shaped to maximize exposed surface area in order to increase energy capture. Additionally, the top side float volume, or freeboard F1, is optimized to the minimal necessary volume (i.e. reduced freeboard) to allow sufficient driving force while eliminating excess reserve buoyancy to improve survivability. This contributes to a continued operation of the WEC 10 in all wave conditions (including storm waves) by removing excess force that would otherwise be created by excess freeboard.

[0053] FIG. 6 depicts one embodiment of the aft float 20. The aft float 20 comprises an aft arm 21a, the length of which is selected for optimum power extraction in a target wave climate. FIG. 7 depicts the aft float 20 with no aft arm 21a formed thereon or otherwise attached thereto. The rotatable aft float 20 is designed in one embodiment with a deep draft D1. The depth of the draft D1 is optimized to maximize surface area which is in contact with the wave. The exposed surface is maximized to increase energy capture when the wave force acts against

the rotatable aft float 20. The top side 22 of the rotatable aft float 20 is designed to minimize materials (i.e. reduce costs) used to enclose the structure. For example; completing the structure with a semicircle requires more material and increases cost. All sides (e.g. top side 22, front side 23 and left side 24) of rotatable aft float 20 are slightly convex rather than flat. This slight curvature is designed to allow for composite manufacture on a wound mandrel. The curvature also allows for composite manufacture processes that use a mold.

[0054] The front surface 23 of the rotatable aft float 20 faces toward the oncoming wave and is optimized in both radius and slope in order to maximize energy capture from the incident wave climate. Hydrodynamic numerical analysis and optimization techniques were employed to design the rotatable aft float 20 to maximize power delivered from the rotatable aft float 20 while minimizing the material utilized. Thus this shape (slope and radius) is the result of an optimized power to cost ratio. In a plan view perspective, the front surface 23 of the rotatable aft float 20 is rectangularly shaped to maximize exposed surface area in order to increase energy capture. Additionally, the top side float volume, or freeboard F2, of the rotatable aft float 20 is optimized to the minimal necessary volume (i.e. reduced freeboard) to allow sufficient driving force while eliminating excess reserve buoyancy to improve survivability. This contributes to a continued operation of the WEC 10 in all wave conditions (including storm waves) by removing excess force that would otherwise be created by excess freeboard.

[0055] FIG. 8 depicts the embodiments of the fore float 15 of FIG. 5 and the aft float of FIG. 7 in oriented relative to one another as if engaged with a nacelle 25. The optimized shape of the aft float 20 is similar in outer contour to that of the fore float 15. In one embodiment, this similarity allows for both the fore float 15 and aft float 20 to be made from the same mold and manufacturing process, thus reducing manufacturing costs. To utilize a fore float 15 as an aft float 20, the fore float is flipped from port to starboard and rotated toward the bottom as seen by tracking point "A". This allows for cost reductions by making both floats from a single mold.

[0056] Turning now to the features of the nacelle 25 as depicted in FIGS. 1 and 2, the nacelle 25 has a relatively large diameter 27. The length 28 of the nacelle 25 extends the full width of the fore float 15 and aft float 20 which increases the surge response of nacelle 25. Increased surge motion of the nacelle 25 results in increased relative pitch motion and driving force between fore float 15 and the nacelle 25, and between the aft float 20 and the nacelle 25. The result of this design is indicated in the embodiment of the WEC 10 in FIG. 9. These forces

and motions have been enhanced through optimization of hydrodynamic shape (e.g. cylindrical) and size (e.g. large diameter of approximately 9meter). A large diameter nacelle allows for the design and use of unique large diameter permanent magnet generators (not shown) housed therein while reducing cost of manufacture for both a bearing/sealing system and generator. Additionally, returning to FIGS. 1 and 2, the large diameter 27 and high mass of the nacelle 25 combined with a rescinding freeboard allows for an improved phase relationship between the fore float 15 and nacelle 25 and the aft float 20 and nacelle 25. Furthermore, the cylindrical shape of the nacelle 25 allows for cost effective composite manufacturing using a mandrel or using a rolled steel process.

[0057] The nacelle 25 encloses a plurality of power takes offs for capturing wave energy. The plurality of power take offs may include, for example, all forms of rotary power conversion, such as a large direct driven rotary (DDR) electric generator, a gear box driven electric generator, a belt driven electric generator, water pumping systems, water desalination, pneumatic pumping systems and even hydraulic pumps, and similar devices. In one embodiment, the WEC 10 includes a first DDR permanent magnet generator (PMG) (not shown) and a second DDR PMG (not shown). The first DDR PMG and second DDR PMG are disposed concentrically with the longitudinal central axis and at opposing ends of the nacelle. The rotatable fore float 15 has at least one fore arm 16a that interconnects with a drive shaft (not shown) the first DDR PMG through a sealed bearing (not shown). The rotatable aft float 20 has at least one aft arm 21a that interconnects with a drive shaft (not shown) of the second DDR PMG through a second sealed bearing (not shown). The fore arm 16a is depicted at least in FIGS. 1, 2 and 6. The aft arm 21a is depicted at least in FIGS. 1, 2, and 7. FIG. 3 depicts the rotatable fore float 15 and rotatable aft float 20 relative to the nacelle 25 with the fore arm 16a and aft arm 21a removed. The fore arm 16a and aft arm 21a are designed to drive their respective generators. In one embodiment, the rotational fore float 15 also includes an idle arm (not shown) and the rotational aft float 20 includes an idle aft arm 21b, wherein the idle arms rotatably mount to the end of the nacelle 25 opposite the end to which the drive arms 16a, 21a are mounted. This enables a secure and balanced rotatable mounting of the fore float 15 and aft float 20 to the nacelle 25.

[0058] The floats 15 and 20 of FIG. 1 experience horizontal forces and due to wave surges shown in FIG. 2 and, under this application of force, the floats 15 and 20 rotate with respect to the spar 30. The surge forces are minimal at the bottom of the spar 30 and at the

damper 35. This difference in horizontal loading between the top of spar 30 and the bottom of that spar 30 causes a moment about the spar body, so as to cause the spar to pitch to the left or right of a vertical orientation. The WEC 10 bodies including the fore float, aft float and the unit formed by the mated damper 35, spar 30, and nacelle 25 are ballasted with controllable balance for optimal energy extraction during different seasons, thereby accommodating predictable changes in wave force. The ballast design also achieves a desired center of gravity 40 along the length of the spar 30. This location of the center of gravity 40 affects the speed of the pitching action and the amount of energy absorbed by the rotatable nacelle 25, rotatable fore float 15 and rotatable aft float 20 and therefore transferred to the first DDR PMG and second DDR PMG.

[0059] The spar 30 includes a center of gravity 40 for the WEC 10 and center of buoyancy (not shown) that contribute to an axis of rotation of the WEC 10 that changes dynamically with any given sea-state or change in ballast. In one embodiment, such as that in FIG. 1, the damper 35 is mounted to the terminal end 33 of a bottom end region 32 of the spar 30 and the center of gravity and center of buoyancy of the wave energy converter are optimized to be between the damper 35 and the water surface 100. In another embodiment, such as that of FIG. 11, the damper 35 is mounted to the bottom end region 32 of the spar at point higher than the terminal end 33 of the bottom end region 32 such that the terminal end 33 extends beyond an underside of the damper 35 and the center of gravity and center of buoyancy of the wave energy converter are between the terminal end of the spar 30 and the water surface.

[0060] Returning to FIGS. 1 and 2, under the application of both surge and heave forces, the floats 15 and 20 rotate about nacelle 25 and transmit power through the respective drive shafts of the first and second DDR PMG. The net affect of these heave and surge driven rotary motions is complementary (not opposing) to the increase in relative motion between nacelle 25 to fore float 15 and nacelle 25 to aft float 20 in direction and force.

[0061] The spar 30 is designed to be out of phase in heave with each float (fore float 15 and aft float 20) so that it resists the upward and downward heave motion of the floats. The spar 30 may also be designed such that it has a ballast chamber therein (not shown) that varies the spar buoyancy between either positively buoyant when the wave trough is above the spar, or negatively buoyant when the wave crest is above the spar. Spar 30 is designed to transition between positive buoyancy and negative buoyancy, while maintaining the buoyancy of the WEC 10 to avoid sinking. This transitional buoyancy causes the heave motion of the spar 30 to move

opposite (180 degrees out of phase) to the heave motion of the rotatable fore float 15 and rotatable aft float 20. This diving and rising spar design is accomplished using a compressible ballast chamber in the lower section of the spar (not shown). When the wave crest is over spar 30, the higher pressure from the wave causes the ballast chamber to compress and causes the spar 30 to sink until the floats reach equilibrium buoyant state. Conversely, when the wave trough is over spar 30, the pressure on the buoyancy chamber is reduced, the ballast chamber expands, and spar 30 rises until the rotatable fore float 15 and rotatable aft float 20 reach an equilibrium buoyant state with the spar 30. This diving and rising action amplifies the range of motion between the rotatable fore float 15 and rotatable aft float 20 and the spar 30, and thereby improves performance of the WEC 10. Ballasting the spar 30 increases captured power and optimizes relative rotational speed between the spar 30 and the rotatable fore float 15 and rotatable aft float 20.

[0062] The geometry of components of the WEC 10 can be optimized for use on different bodies of water during different seasons based on many factors. The fore float 15 and aft float 20 may be constructed with a narrow width to length ratio, or with a wide aspect ratio. Fore float 15 and aft float 20 geometry is optimized for wave height, wave period, seasonal wave spectral density, power capture, and directionality considerations. The shape of the rotatable fore float 15 and rotatable aft float 20 is not limited by the geometry heretofore described. The rotatable fore float 15 and rotatable aft float 20 also might be, for example, cylindrical or rectangular in shape, and the length of the fore arm 16 and aft arm 21 may vary to suit the water conditions or to control the amount of energy being absorbed. Similarly, the diameter or length of the spar 30 may be altered for performance enhancements.

[0063] Embodiments of the present invention consider buoyancy and freeboard volumes. The fore float 15 and aft float 20 of FIG. 1 are designed to provide maximum generator driving torque, thus optimizing the integrated float and generator design. To achieve this, the maximum freeboard volume of fore float 15 and aft float 20 is controlled. For example, as shown in the embodiment of FIG. 9, the volume of the WEC 10 above the surface is kept low to prevent excessively high forces and torques from acting on the WEC 10. This improves the survival characteristics of the WEC 10. The fore float 15 first angle of attack  $\alpha_1$  and aft float 20 second angle of attack  $\alpha_2$  with respect to the incoming wave is optimized to maximize power extracted. In one embodiment depicted in FIG. 9, the first angle of attack  $\alpha_1$  is 32.62 degrees and the aft

float 20 angle of attack  $\alpha_2$  is 52.38 degrees. These depicted volumes and dimensions are representative of an exemplary full scale WEC 10 being 27 meters long L and having a fore float 15 freeboard height F1 of 1.36m, an aft float 20 free board height F2 of 1.61 meters and a nacelle 25 freeboard height F3 of 2.50 meters. The ratio between submerged and above surface volume is used to control the phase relationship between the fore and aft floats 15, 20 and the spar 30. Designing the fore and aft floats 15, 20 and spar 30 to have an opposite phase relationship improving relative motion between the fore and aft floats 15, 20 and spar 30 and thereby increases energy capture.

[0064] In one embodiment, a two point mooring system (not shown) is used to control directionality of the WEC 10 and therefore the rotatable fore float 15 and rotatable aft float 20. The WEC 10 may be slack moored, having a slack mooring line that attaches to the nacelle 25 or damper 35. A mechanism such as a chain winch can be used to shorten or lengthen either mooring lines, thereby rotating the WEC 10. In another embodiment, a three point mooring system is used to control directionality. This system may be slack moored such that the lines join to the damper 35 at a common connection point. As shown in FIGS. 10-12, one embodiment of the WEC 10 may have yaw control system 37 disposed on the damper 35 and designed to provide for directional orientation of the WEC 10 within its mooring. It is also possible to add a keel 36 to the underside of the damper 35. The keel 36 provides roll stability by reducing roll motion in directionally spread seas. This same keel 36 when aligned parallel to the wave front can be used as a drag plate to increase pitch motion of the spar 30 and increase performance.

[0065] Accordingly, in another aspect, the present invention includes methods for generating power using the WEC 10. In one embodiment, the method includes providing a rotational fore float having a first angle of attack relative to the horizon and a rotational aft float having a second angle of attack relative to the horizon. The method includes providing a sealed nacelle enclosure having a central longitudinal axis at both ends of which are disposed a drive rotary generators, a first direct drive rotary generator being mechanically coupled to the first rotational float and a second direct drive rotary generator being mechanically coupled to the second rotational float. The method includes providing a spar having a top end mated with the nacelle and a bottom end mated with a heave plate, wherein the spar and damper extend into a body of water while the first rotational float and said second rotational float are supported at the water surface such that wave heave and wave thrust rotate the first rotational float and the second

rotational float in opposite directions about the central longitudinal axis. The method further includes assembling a wave energy converter unit by attaching the first rotational float and second rotational float to the nacelle and attaching the nacelle to the spar; and deploying the wave energy converter within a fluid flow of waves.

[0066] As an electrical generating system, the WEC 10 offers a reduced cost of energy (CoE) advantage over other approaches. Computer modeled simulations, such as the exemplification included herein, led to a design of the WEC 10 depicted in FIGS. 1 and FIG. 14, which extracts 2 to 3 times more wave energy than the prior art embodiment 200 depicted in FIG. 14. The WEC 10 has the potential to be half the size of a competing wave energy converter of the same power rating. That size reduction reduces capital costs and CoE. The CoE is further reduced by reducing the capital expenditure of the generator by optimizing the electromagnetic design using a large diameter generator when low-speed high-torque rotary motion is employed. Operating and maintenance costs are reduced by the operational design; The WEC 10 contains minimal moving parts, and the parts that do move do so fluidly with the incoming waves, so as to reduce the affect of snap loading often experienced by marine deployed bodies. This construction and approach reduces repair time and cost. The speed of rotation and driving torque are both increased by the extraction of both heave and surge energy. Increasing the speed of body motions (e.g. fore float 15 and aft float 20) helps to reduce generator capital costs, and the WEC 10 system components may be designed to satisfy this priority. In some method, reliability is improved by the elimination of all intermediate conversion stages. The WEC 10 Survivability is another advantage of this system. The combined effect of the design results in a fluid motion of the WEC 10 in the ocean which reduces structural loading, reduces mooring loading, and accommodates for tidal variation.

[0067] These methods described utilize rotary motion from a WEC 10 to allow for a point absorber design that captures the heave and surge energy components of the incoming wave energy. By capturing both the surge and heave component, the maximum possible energy capture width of the wave energy device is  $\lambda/\pi$  (where  $\lambda$ =wave length) as compared to  $\lambda/2\pi$  for a device that captures only the heave component. This improvement in capture width is expected to reduce the size and cost of the wave energy converter.

[0068] Overall draft, center of gravity, and moment of inertia for each of the floats 15, 20 and nacelle 25/spar 30 body are individually optimized for optimum performance in the target

wave climate. This is achieved by adjusting both fixed ballast and/or variable ballast tanks in each of the WEC bodies, the fore float 15, aft float 20, nacelle 25 and spar 30.

[0069] Numerical analysis shows that ballast adjustments can be made to achieve optimum performance in differing wave climates. Operationally and by design, this translates to a variable ballast system that allows for the WEC 10 to be tuned for optimum energy capture. This WEC 10 may use a variable ballast system comprised of ballast tanks, control valves, compressed air and pumped water to achieve an automatically controlled variable ballast system.

[0070] The WEC 10 body design optimization includes a cost function for materials and manufacturing. The WEC 10 design optimization includes generator torque-speed performance feedback and the costs associated with the generator materials and manufacturing costs. The integration of hydrodynamic optimization, torque-speed optimization and cost reduction define the complete system shapes, centers of gravity and inertias.

[0071] Bodies (floats 15, 20, spar 30, nacelle 25) of this WEC 10 are designed for manufacture using a mandrel to reduce the cost of manufacture while still allowing for improved performance. Performance is also optimized by adjusting the WEC heading into the wave. This may be achieved through any number of Yaw control systems; any of which may be used by this design.

[0072] It is noted that the foregoing examples have been provided merely for the purpose of explanation and are in no way to be construed as limiting of the present invention. While the present invention has been described with reference to an exemplary embodiment, it is understood that the words, which have been used herein, are words of description and illustration, rather than words of limitation. Changes may be made, within the purview of the appended claims, as presently stated and as amended, without departing from the scope and spirit of the present invention in its aspects. Although the present invention has been described herein with reference to particular means, materials and embodiments, the present invention is not intended to be limited to the particulars disclosed herein; rather, the present invention extends to all functionally equivalent structures, methods and uses, such as are within the scope of the appended claims.

[0073] EXEPLIFICATION

[0074] To arrive at the embodiment of the design of the WEC 10 depicted in FIG. 13, 1300 hours of simulations were run to compare WEC 10 designs (e.g. fore float 15 and aft float 20 geometries, angles of attack and orientations) to the prior art design 200. For each WEC 10 design, the energy capture was predicted over 5 different wave climates throughout the world and the final design behaved the most efficiently under all climate conditions. FIGS. 21-42 depict the details of an exemplary The following AQWA Simulation Narrative describes the process of taking hydrodynamic results from AQWA computer modeled simulations and making calculations to aid in comparisons made between competing WEC 10 shapes, mass matrices, damping values, and torque limits. This process was also used to simulate the affects of mooring arrangements, directionality, making performance predictions, and assisted in making COE estimates. Matlab was the primary platform used to post process AQWA results and execute this process.

[0075] I. RAOs from AQWA

[0076] AQWA provides frequency dependent RAOs for each body in the X, Y, Z, RX, RY, and RZ directions as depicted in FIG. 14. The RAO's provide magnitude and phase data for each structure and every damping setting based on a 1 meter amplitude regular wave input. RAOs are then processed into the relative velocities and torques between floats and spar. Scaling these per meter RAOs by wave height provides all the needed data for power calculation. The best damping case for each dominant wave period and height are systematically selected to produce an active control map, described in section V.A. The RAO's resulting from the active control RAO's are plotted on page 3 of the Comparison Template and include, pitch, heave, relative velocities and torque RAO. Among these, there is an important phase relationship that is of interest, the phase difference between the floats' pitch and spar heave as shown in FIG. 15. These two plots indicate whether the pitch of the floats and the heave of the spar are in-phase or out-of-phase respectively. Ideally, both floats would be out-of-phase with the spar to obtain maximum velocity at articulation point. The desired out-of-phase relationship is shown as the dashed green guide line, were in-phase is in red. The guide lines are switched between the Fwd and Aft floats due to the sign convention between their rotations.

[0077] A. Damping Settings

[0078] Both Fwd and Aft damping are swept through 6 values to create a 6x6 matrix for a total of 36 damping combinations. WEC performance for each of the 36 damping cases (*damp*) is simulated in AQWA for every *Hs* and *Tp*.

Table 1.

Fwd Damping (Nms/rad)	Aft Damping(Nms/rad)
1,202,600	1,202,600
3,269,000	3,269,000
6,077,600	6,077,600
8,886,100	8,886,100
16,520,600	16,520,600
24,155,000	24,155,000

[0079] B. Torque Limit

[0080] A torque limit is imposed on the torque RAOs in order to represent a physical limit of the Direct Drive generator. Data taken from tank testing was used to generate a plot of the average power level versus an imposed torque limit that was swept for all winter wave climates. FIG. 16 shows an example of this average power versus max torque plot showing the *Tmax* value at the transition point in the curve, all climates have similar results. The maximum damping value based on generator efficiency limits, resulting in an  $\omega_{T_{max}}$  at which *Tmax* is achieved.

$$T_{max} = 4,106,350 \text{ Nm}$$

$$Max \text{ Damping} = 24,155,000 \text{ Nms/rad}$$

$$\omega_{T_{max}} = 4,106,350 \text{ Nm} / 24,155,000 \text{ Nms/rad} = 0.17 \text{ rad/s}$$

[0081] The torque RAO's [Nm/m] are multiplied by the wave height axis values in order to generate a four-dimensional table of torque(*H,T,damp*) in units of [Nm]. This creates torque values which exceed the Direct Drive maximum torque capabilities. To overcome this discrepancy the values from the torque table were limited to  $T_{max}$  as shown in FIG. 17.

[0082] II. Power Calculations

[0083] These calculations are used for regular wave RCW calculations described in section III.

[0084] A. WEC Power ( $P_{WEC}$ )

[0085]  $P_{WEC}$  is calculated directly from RAO's values of relative velocities and torques. Each RAO based on a 1 meter amplitude input wave modeled in AQWA is multiplied by the wave height axis to give 4D RAO's based on  $T$ ,  $H$ , and *damping*. For WEC power predictions, the torque limit 4D torque RAO is used. Since RAO values are peak values, each is divided by  $\sqrt{2}$  to give RMS values.

$$P_{WEC\_regular}(T, H, damp) = \frac{\tau_{RAO}(T, H, damp)}{\sqrt{2}} * \frac{\omega_{rel}(T, H, damp)}{\sqrt{2}}$$

[0086] B. Wave Power ( $P_{wave}$ )

[0087] AQWA is run in the frequency domain with 1 meter amplitude regular waves exciting the WEC. The intermediate depth regular wave power equation is used to compute the power from this input wave. The wave power is calculated at a water depth of 55m, the same water depth used in AQWA. The wave power is solved for each period and wave height creating a 3D wave power table at this 55m water depth.

$$P_{wave\_regular}(T, H) = \frac{1}{8} \rho g * c_{g,55m}(T) * H^2 \quad [1]$$

[0088] III RCW Computation in MATLAB

[0089] A family of Relative Capture Width curves is calculated for each of the 36 PTO damping cases based on the 1 meter amplitude input wave. For comparison two distinct RCW families are computed, one using unlimited values for torque the other having the direct drive generator torque limit. The unlimited RCW matrix is presented on pages 1 and 2 of the Comparison Template and noted as uncapped.

[0090] A. Regular RCW

[0091] The WEC power is first divided by the width of the WEC to become the power

per meter width. In the unlimited torque case the wave height does not affect the RCW curve since  $H^2$  is in both the numerator and denominator. Therefore the regular wave RCW calculation can be written in terms of only  $T$  and  $damping$ :

$$RCW_{regular}(T, damping) = \frac{P_{WEC\_regular}(T, damping)}{P_{wave\_regular}(T) * Width}$$

[0092] B. Torque Limited RCW

[0093] Frequency domain modeling assumes torque increases linearly with wave height. We must however consider PTO torque limits for energy predictions. The torque limited RCW is defined based on the 4D torque limited RAO's. This torque limited RCW is used for all subsequent power and energy calculations. The RCW torque limited values are not presented in the figures, but are used for computing power described in IV.D.

$$RCW_{Torque\_Limited\_regular}(T, H, damping) = \frac{P_{WEC\_Torque\_Limited\_regular}(T, H, damping)}{P_{wave\_regular}(T, H) * Width}$$

[0094] IV. Power Spectrum

[0095] A wave power spectrum based on a Pierson-Moskowitz energy spectrum is calculated for each wave climate ( $H_s, T_p$ ) based on the water depth at the specific geographic location.

[0096] A. Two parameter Pierson-Moskowitz spectrum

[0097] A three-dimensional table of spectral energy data is created for each wave climate based on  $H_s$  and  $T_p$ . This table is of the same dimensions as the Occurrence Table defined later in section IV.G. The energy spectrum  $S(T_p, H_s, f)$  is derived from the two parameter Pierson-Moskowitz equation:

$$S(T_p, H_s, f) = A \left(\frac{f}{f_p}\right)^{-5} * \exp\left(-B \left(\frac{f}{f_p}\right)^{-4}\right) \tag{2}$$

where,  $A = \left(\frac{1}{2} H_s^2\right) * B$   
 and,  $B = \frac{5}{4} (T_p)^{-4}$

[0098] B. Group Velocity ( $c_g$ )

[0099] Group velocity describes the rate that wave energy is transmitted by the wave, it is a water depth ( $h$ ) dependent value, and must be recomputed for every wave climate.

$$c_p(f, h) = \left[ \frac{1}{2} + \left( \frac{kh}{\sinh(2kh)} \right) \right] * c \tag{1}$$

Solve for c for each period:  $c(f, h) = \frac{gT}{2\pi} \tanh(kh)$

Solve for k for each period and water depth:  $(2\pi f)^2 = gk * \tanh(kh)$

[00100] C. Convert Energy to Power

[00101] As depicted in FIG. 18, for every  $H_s$ ,  $T_p$ , and  $h$ :

$$P_{\text{wave}} \text{ [W/m]: } I = \rho g \int_0^\infty c_p(f) * s(f) df \tag{2}$$

[00102] D. Average WEC Power ( $P_{\text{WEC\_spec}}$ ) from Spectrum

[00103] The first step to computing WEC power is to align the torque limited

RCW ( $RCW_{\text{Torque Limited}}$ ) with the raw wave power ( $P_{\text{wave}}$ ) by first converting

$RCW_{\text{Torque Limited}}(T, H, \text{damp})$  to the frequency axis form  $RCW_{\text{Torque Limited}}(f, H, \text{damp})$ .

To calculate the average power absorbed by the WEC in each wave case ( $H_s$ ,  $T_p$ ), and for each damping case, multiply the raw wave power ( $P_{\text{wave}}$ ) by the  $RCW_{\text{Torque Limited}}$  for each damping case at the given  $H_s$ .  $RCW_{\text{Torque Limited}}(H_s)$  represents the RCW with the appropriate generator torque limiting action. Solving this for each damping case gives a family of average powers per available damping case for every  $H_s$ ,  $T_p$ ,  $h$  and damping:

[00104] Absorbed Power [Watts]:

$$P_{\text{WEC\_spectrum}} = \text{Width} * \rho g \int_0^\infty [c_p(f) * s(f) * RCW_{\text{T Limited}}(f, H_s)] df$$

[00105] Where  $RCW_{\text{T Limited}}(H_s)$  is the torque limited RCW at  $H_s$ .

[00106] E. Find the Active Damping Setting

[00107] The average power levels are compared and the damping case that provided the highest average power level is chosen as the active damping setting for each  $T_p$ ,  $H_s$ , and water depth ( $h$ ). FIG. 19 is a color scale map example of the best damping cases (index) that were used for the given climate. The best damping cases (1 to 36) were modeled for Oregon wave climate at a water depth of 123 m.

[00108] V. Energy Predictions

[00109] A. Occurrence Table

[00110] The Occurrence Table = is a statistical representation of wave data that lists the number of hours per year that each wave condition ( $H_s, T_p$ ) occurred in a given wave climate. FIG. 20 shows an example for Oregon, plotted with the annual energy in the color scale

[00111] B. Annual Energy Estimation

[00112] The total annual energy is calculated by multiplying active power for each  $T_p$  and  $H_s$  with the number of hours each  $T_p$  and  $H_s$  occurred annually from the Occurrence Table. This creates an energy table representing the total energy produced by each  $T_p$  and  $H_s$  annually, seen in Figure 6 in color scale. This table is then summed with a double integral into a single number representing the estimated energy produced from the given wave climate.

$$E_{\text{annual}}(h) = \iint [P_{\text{WEC, spectrum}}(T_p, H_s, h) \cdot \text{occurrence table}(T_p, H_s, h)] dT_p dH_s$$

[00113] C. Spectral Energy

[00114] By taking a single integral of the previously mentioned energy table in the  $H_s$  direction we get a 2D spectral energy curve representing an annual estimate of total WEC absorbed energy for each dominant period  $T_p$ .

$$E_{\text{WEC}}(T_p, h) = \int [E_{\text{WEC}}(H_s, T_p, h)] dH_s$$

[00115] A similar summation can be made with the raw wave energy in a given wave climate resulting in a curve estimating energy per  $T_p$ .

$$E_{\text{waves}}(T_p, h) = \int [E_{\text{waves}}(T_p, H_s, h)] dH_s$$

[00116] These two spectral energy curves are presented on page 4 of the

Comparison Template for each of the 8 wave climates that are being investigated. Having both the spectral WEC absorbed energy and spectral raw energy which the WEC was exposed to; we are able to define a Power Ratio on the spectral axis for each wave climate. This is seen on page 5 of the Comparison Template report.

$$\mathbf{Power\_Ratio}(T_p, h) = \frac{E_{WEC}(T_p, h)}{E_{wave}(T_p, h)}$$

[00117] Since both the numerator and denominator are products of the Occurrence Table the calculation is equivalent to a power ratio, thus the name. Power Ratio is a unit less term giving an indication of the WEC's ability to absorb power. Power Ratio is symbolic of the WEC capture efficiency over the spectra.

- [1] Dean R.G., Dalrymple R.A., *Water Wave Mechanics for Engineers and Scientists* (97-98) copyright 1991, World Scientific, Singapore
  - [2] Falnes J. *A review of wave-energy extraction*. In: Elsevier Marine Structures 20 (2007) 185-201
- [00118]

## CLAIMS

We Claim:

- 1) A wave energy converter comprising:
  - a) a first rotational float having a first angle of attack relative to the horizon and a second rotational float having a second angle of attack relative to the horizon;
  - b) a sealed nacelle enclosure having a central longitudinal axis at both ends of which are disposed power take offs, a first power take off being mechanically coupled to the first rotational float and a second power take off being mechanically coupled to the second rotational float; and
  - c) a spar having a top end mated with the nacelle and a bottom end region within which a heave plate is concentrically mounted, wherein the spar and damper extend into a body of water while the first rotational float and said second rotational float are supported at the water surface such that wave heave and wave surge forces rotate the first rotational float and nacelle in opposite directions about the central longitudinal axis and the second rotational float and nacelle in opposite directions about the central longitudinal axis.
- 2) The wave energy converter of claim 1 wherein said heave plate and its water surfaces serve to optimize the wave energy converter motions and to accentuate relative motions between the forward float and spar and the aft float and spar.
- 3) The wave energy converter of claim 2, wherein said spar includes a center of gravity and center of buoyancy that contribute to an axis of rotation that changes dynamically with any given sea-state or change in ballast.
- 4) The wave energy converter of claim 3, wherein the heave plate is mounted to the terminal end of the bottom end region of the spar and the center of gravity and center of buoyancy of the wave energy converter are optimized to be between the surge plate and the water surface.
- 5) The wave energy converter of claim 3, wherein the heave plate is mounted to the bottom

end region of the spar at point higher than the terminal end of the bottom end region such that the terminal end extends beyond an underside of the heave plate and the center of gravity and center of buoyancy of the wave energy converter are between the terminal end of the spar and the water surface.

- 6) The wave energy converter of claim 1, wherein the first and second power take offs are low speed, high torque electrical generators comprising stators and windings.
- 7) The wave energy converter of claim 1, wherein the first and second power take offs are one of a generator, gearbox and generator, hydraulics and generator, or a water pump.
- 8) The wave energy converter of claim 2 further comprising a mooring system attached to the heave plate or spar.
- 9) The wave energy converter of claim 2, wherein said heave plate is of generally circular or semi-circular plate-like form.
- 10) The wave energy converter of claim 1, wherein the first angle of attack is between 30 and 35 degrees relative to the horizon.
- 11) The wave energy converter of claim 1, wherein all surfaces of the first rotational float and all surfaces of the second rotational float are convex.
- 12) The wave energy converter of claim 1 wherein the front side of the first rotational float and front side of the second rotational float have a rectangular plan view.
- 13) The wave energy converter of claim 1 wherein the maximum freeboard of the first rotational float is 1.61m.
- 14) The wave energy converter of claim 1 wherein the maximum freeboard of the second rotational float is 1.36m.

- 15) The wave energy converter of claim 1 wherein the height of the portion of the second rotational float beneath a water surface is between 5.25 and 5.75 meters and the height of the portion of the first rotational float beneath the water surface is between 3.75 and 4.25 m.
- 16) The wave energy converter of claim 1 wherein the first rotational float and second rotational float are manufactured from the same mold and manufacturing process.
- 17) The wave energy converter of claim 1 wherein the first rotational float is identical to the second float, and relative to the first rotational float, the second rotational float is flipped 180 degrees from port to starboard and rotated to point downward toward the damper prior to attachment to the nacelle.
- 18) A method for generating power comprising:
- a) providing a first rotational float having a first angle of attack relative to the horizon and a second rotational float having a second angle of attack relative to the horizon;
  - b) providing a sealed nacelle enclosure having a central longitudinal axis at both ends of which are disposed power take offs, a first power take off being mechanically coupled to the first rotational float and a second power take off being mechanically coupled to the second rotational float;
  - c) providing a spar having a top end mated with the nacelle and a bottom end mated with a heave plate, wherein the spar and damper extend into a body of water while the first rotational float and said second rotational float are supported at the water surface such that wave heave and surge forces rotate the first rotational float and nacelle in opposite directions about the central longitudinal axis and the second rotational float and nacelle in opposite directions about the central longitudinal axis; and
  - d) assembling a wave energy converter unit by attaching the first rotational float and second rotational float to the nacelle and attaching the nacelle to the spar; and
  - e) deploying the wave energy converter within a wave field.

19. The method of claim 18, wherein the wave energy converter is oriented such that the central longitudinal axis is perpendicular to the direction of wave travel.

20. The method of claim 19, wherein the wave energy converter is oriented such that said central longitudinal axis is parallel to the direction of wave travel.

21. The method of claim 19, wherein the wave energy converter is oriented such that said central longitudinal axis is neither parallel nor perpendicular to the direction of wave travel.

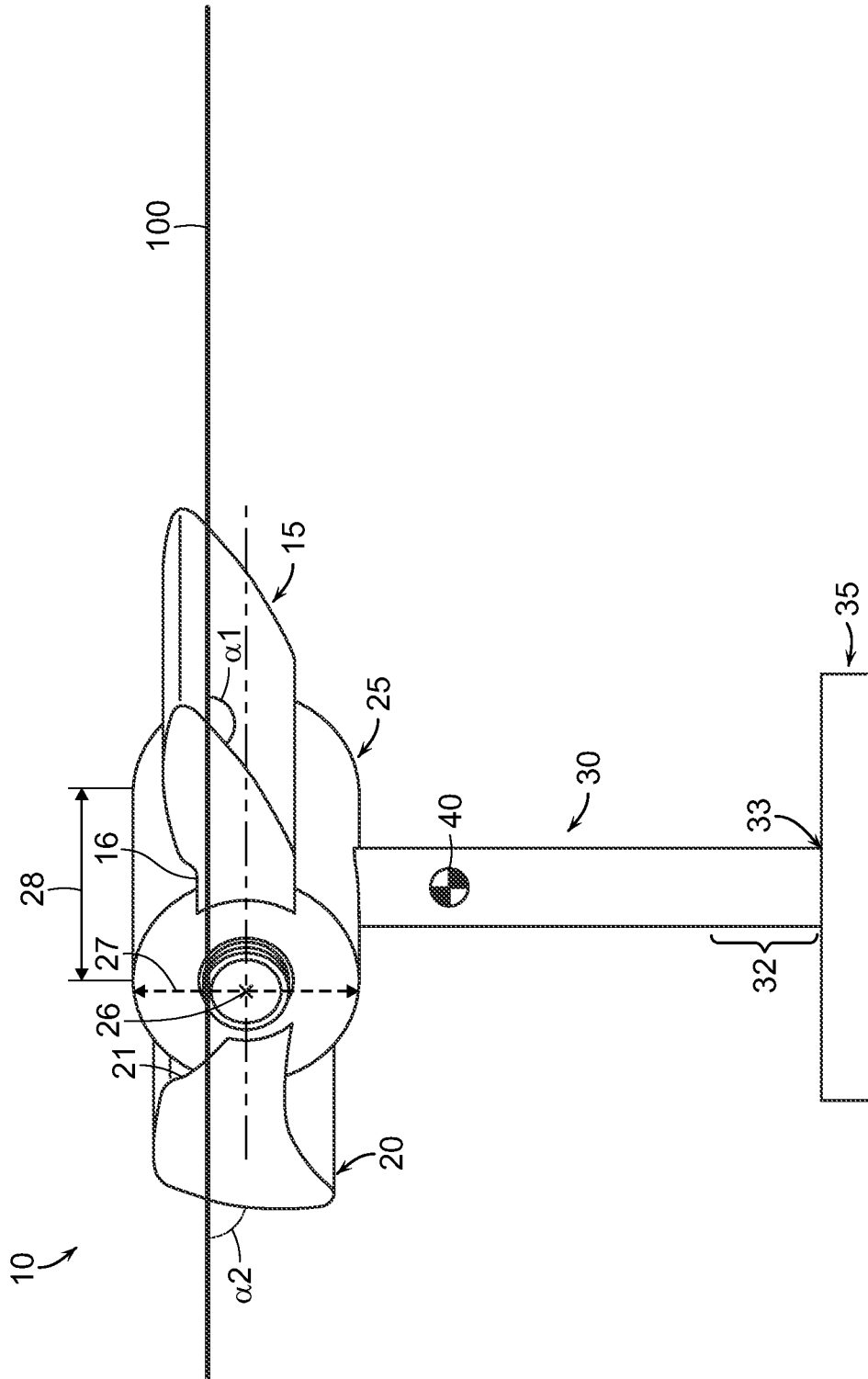


FIG. 1

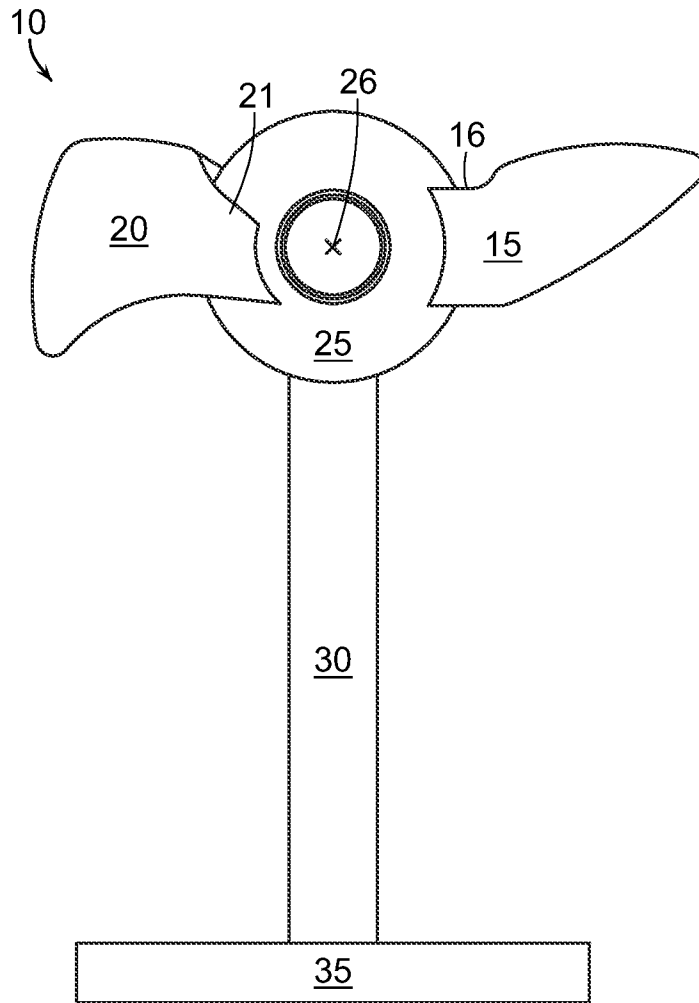


FIG. 2

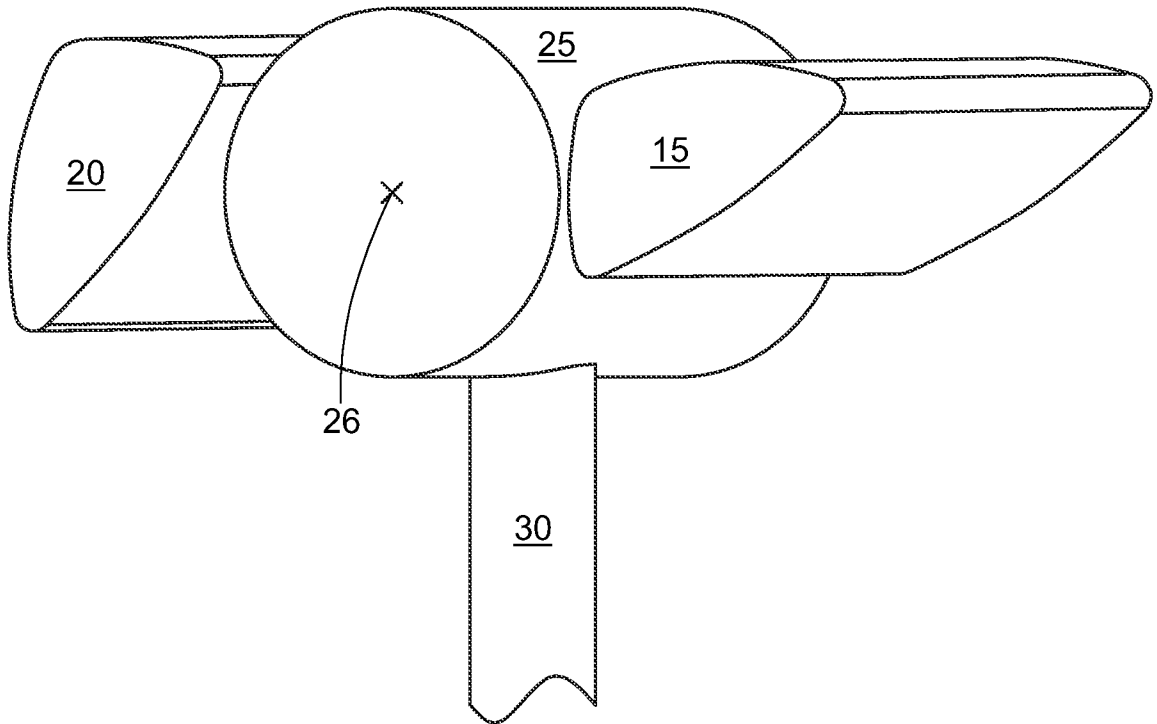


FIG. 3

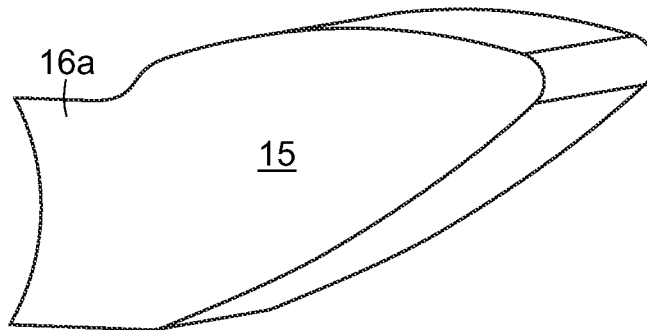


FIG. 4

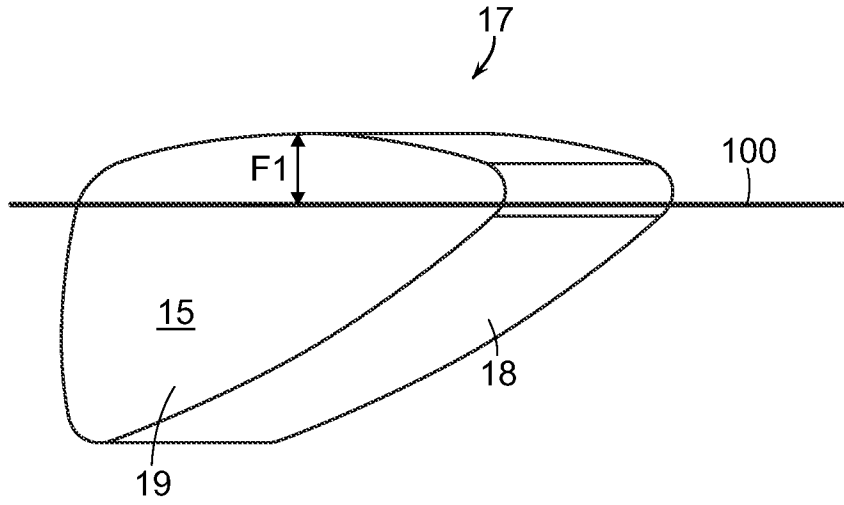


FIG. 5

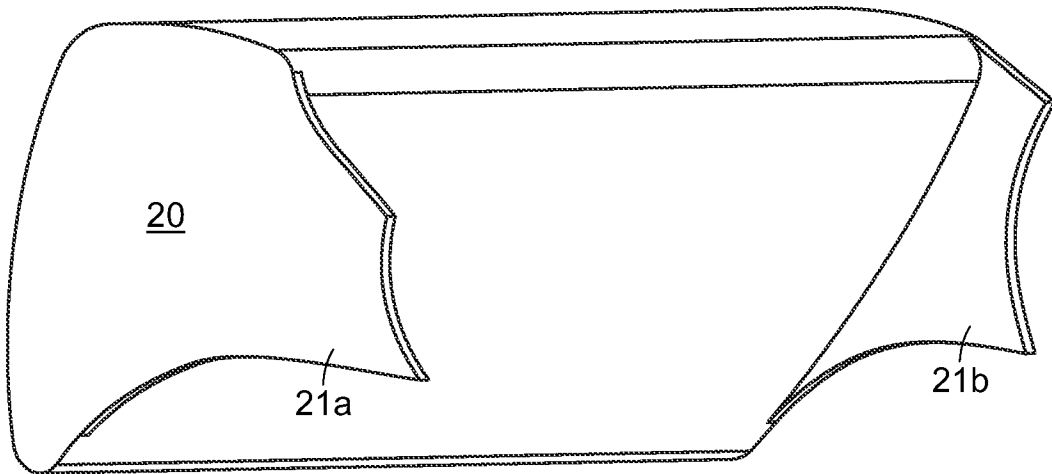


FIG. 6

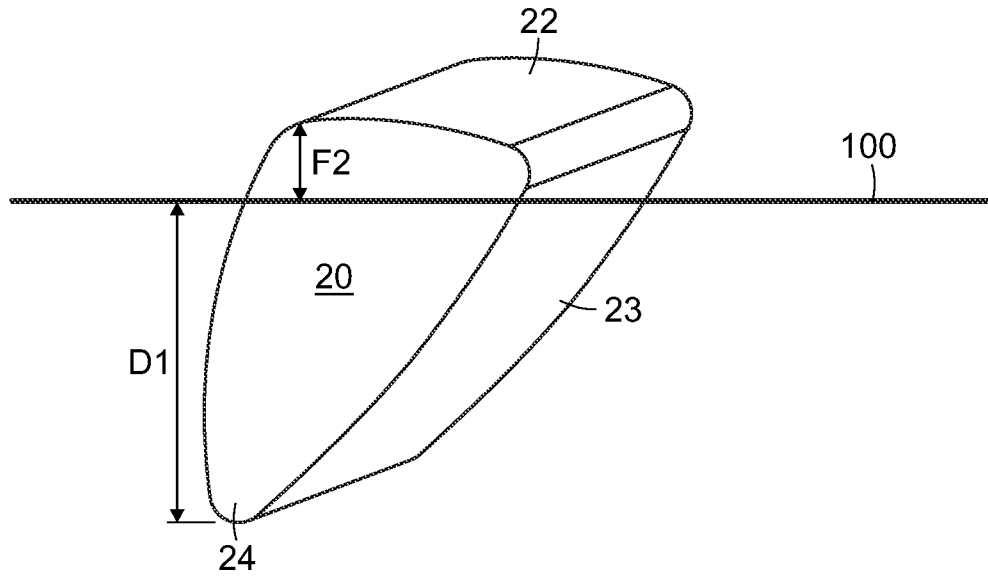


FIG. 7

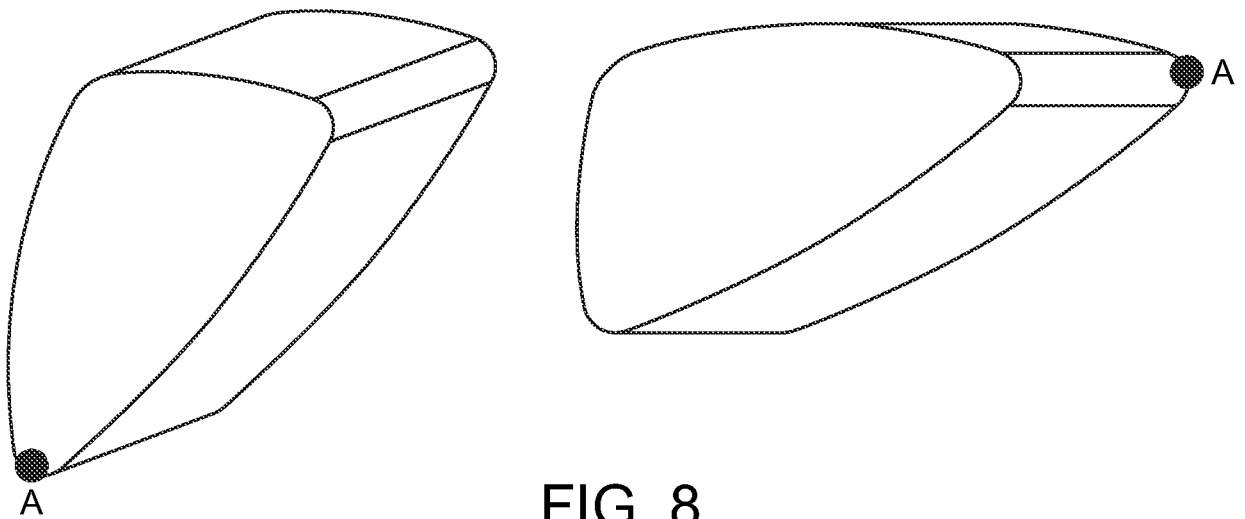


FIG. 8

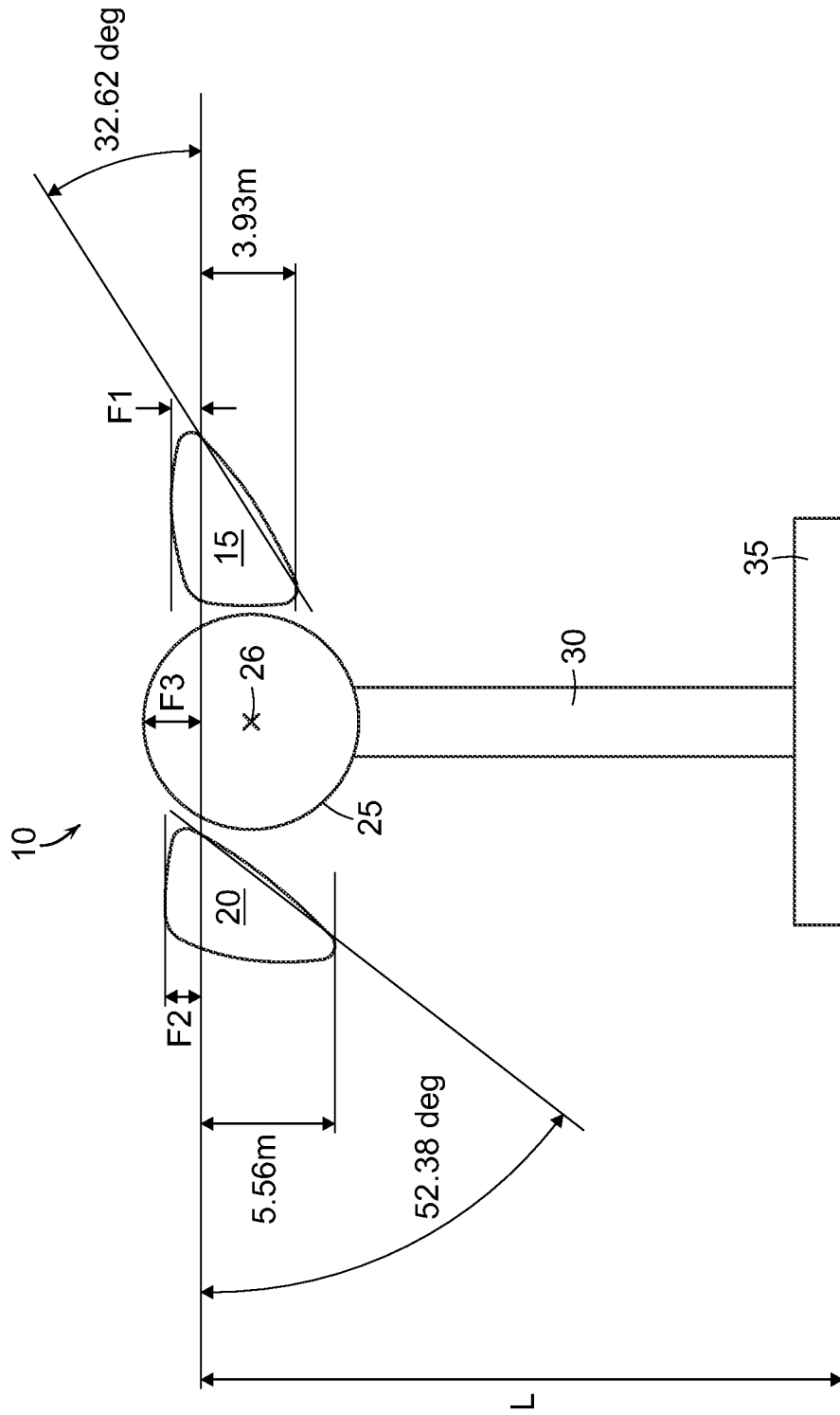


FIG. 9

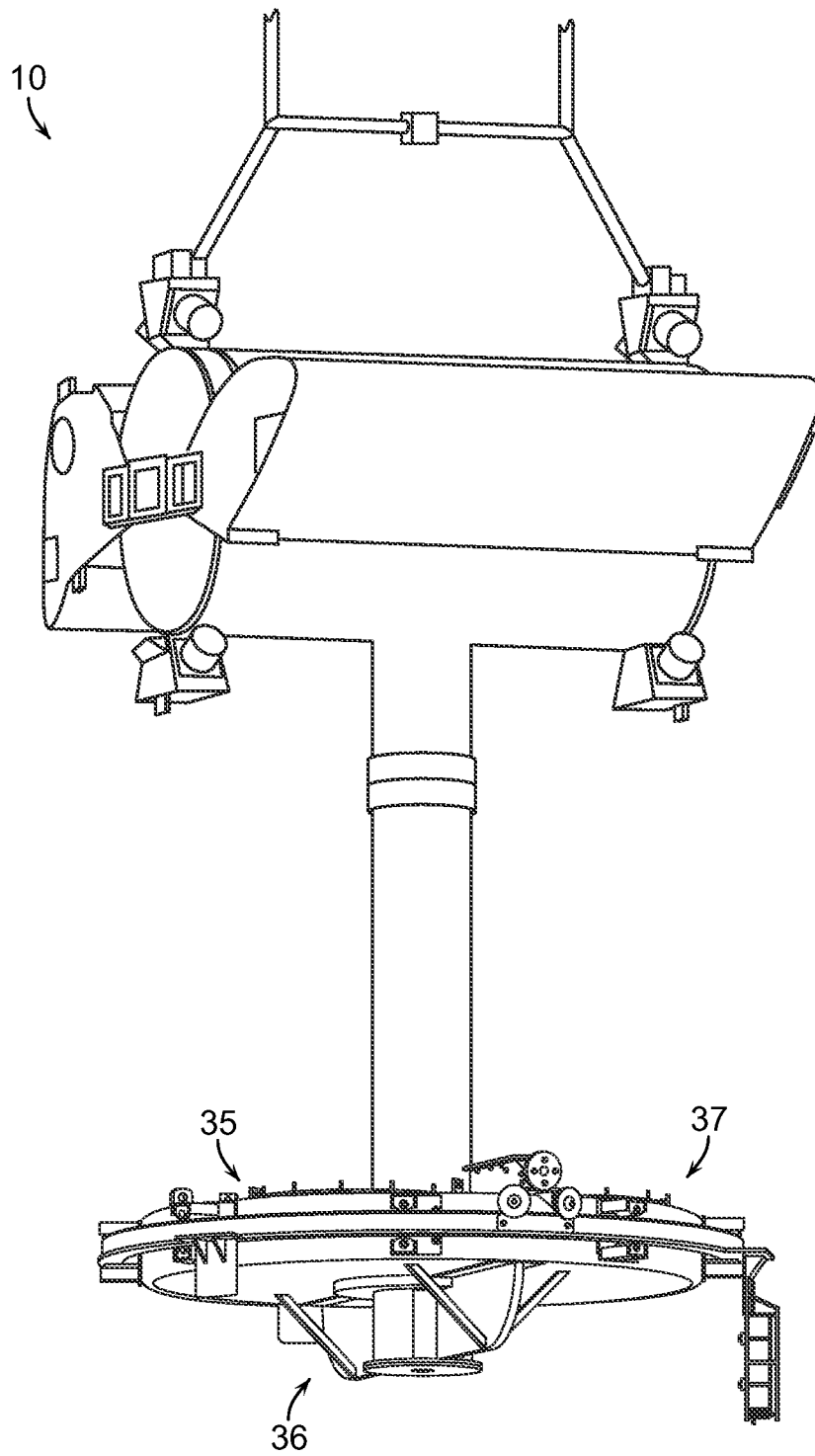


FIG. 10

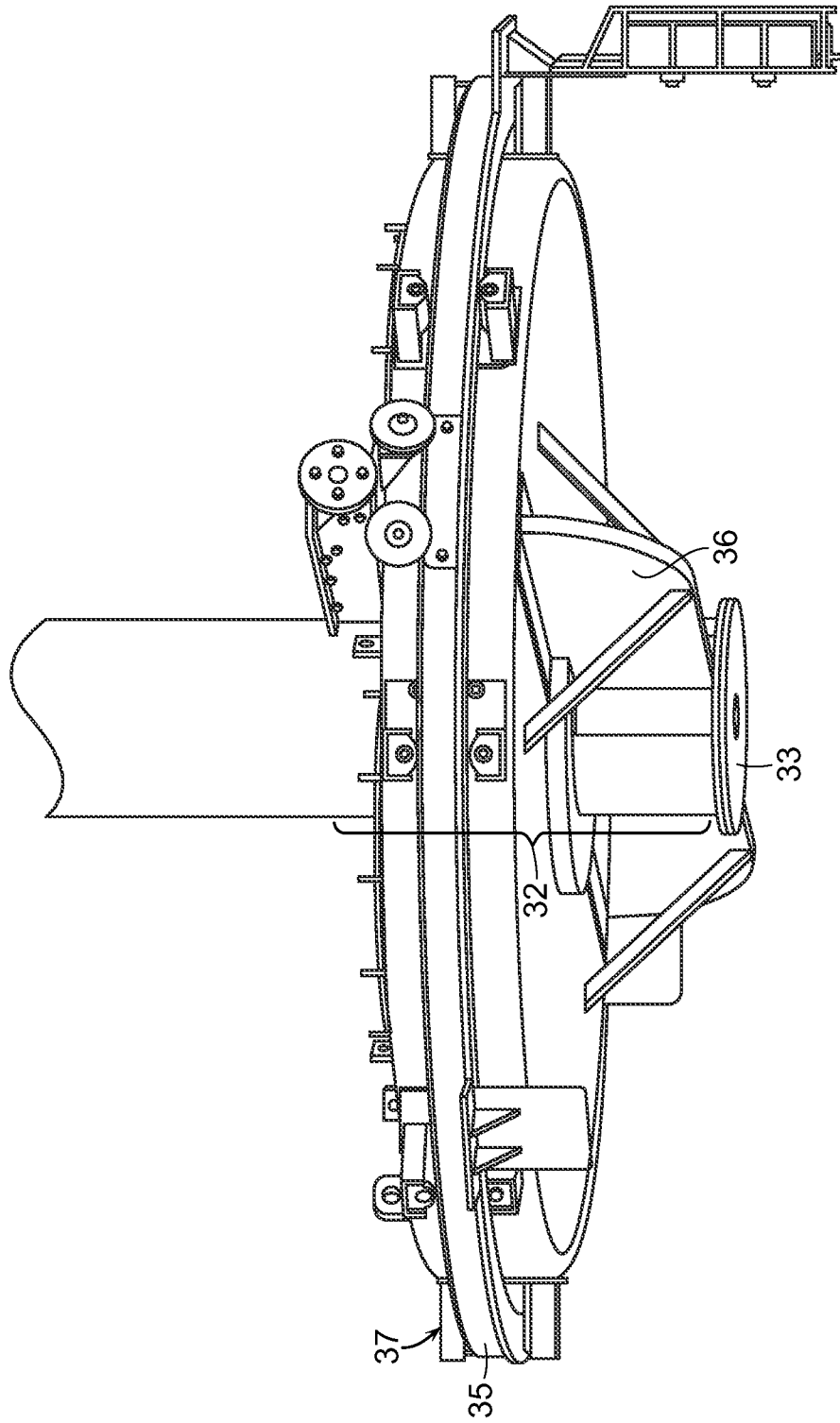


FIG. 11

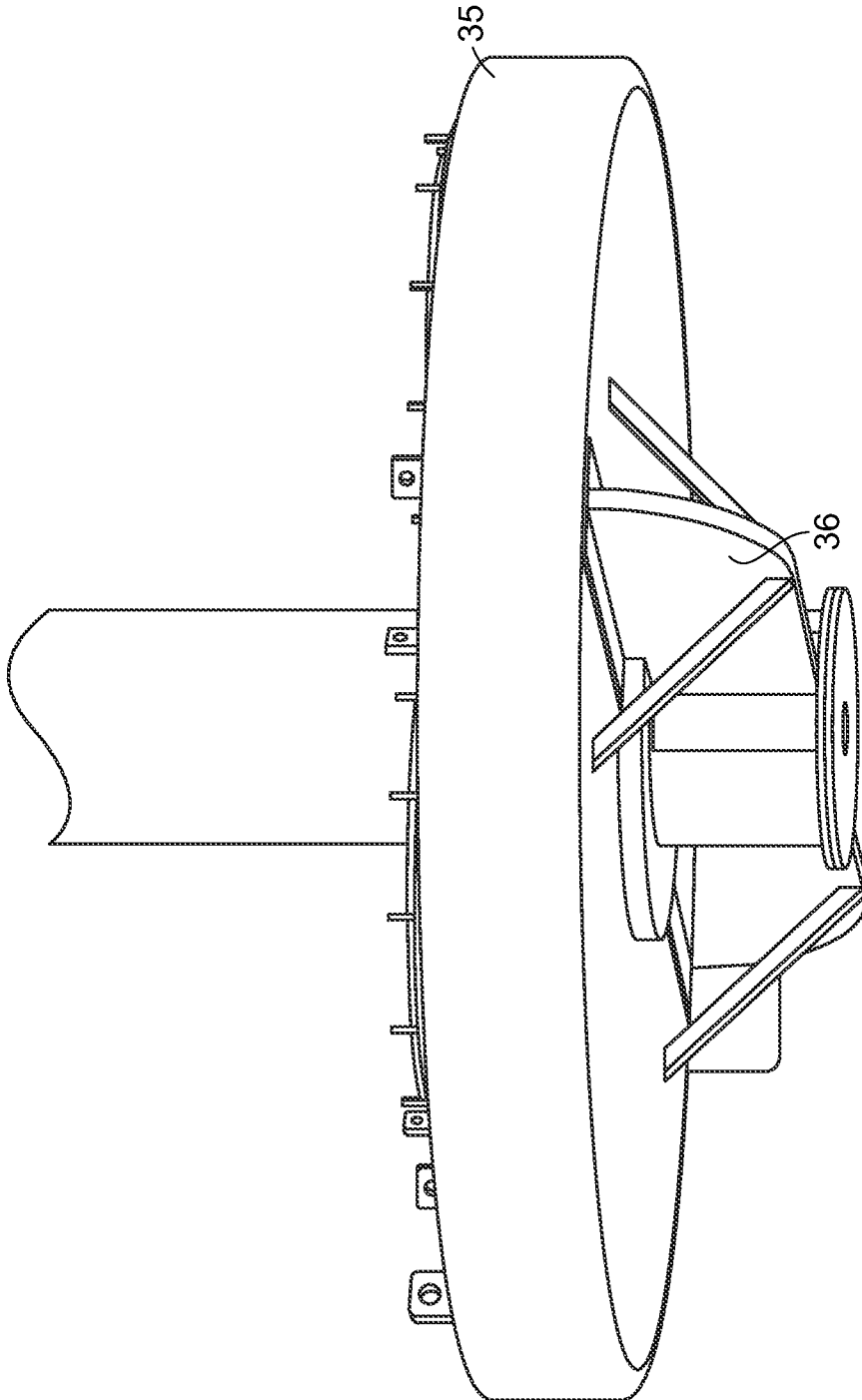


FIG. 12

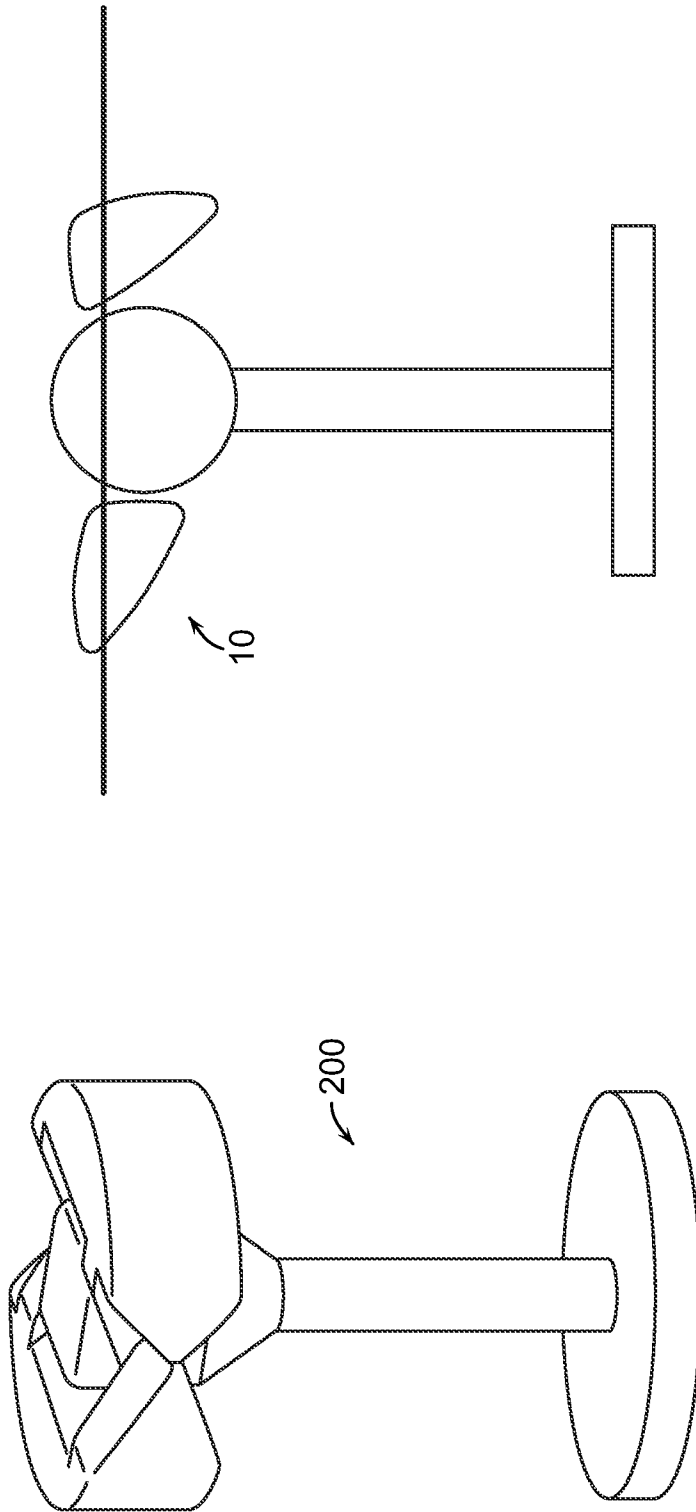


FIG. 13

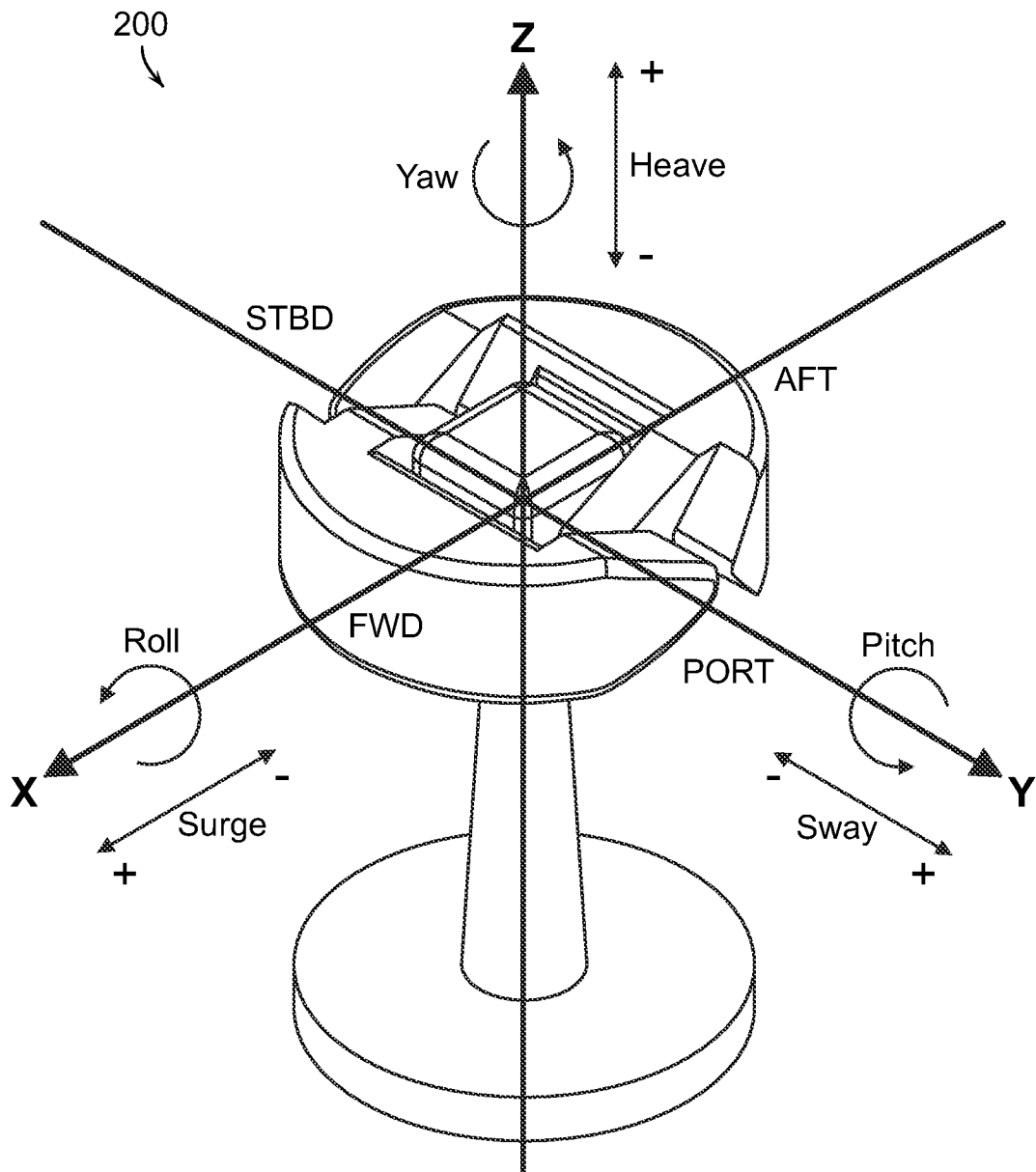


FIG. 14

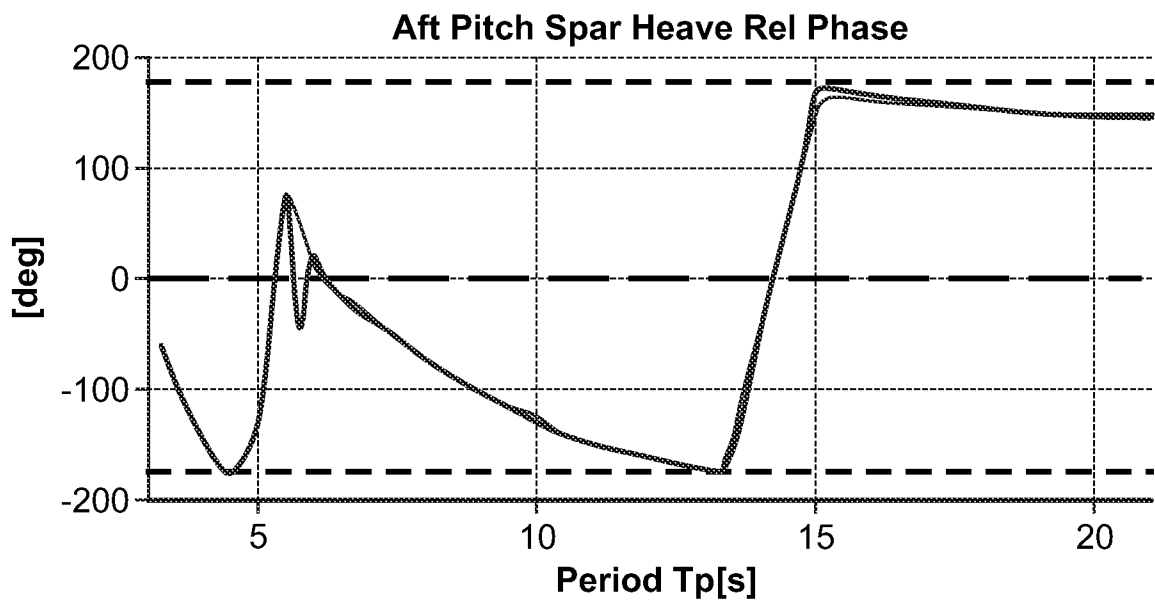
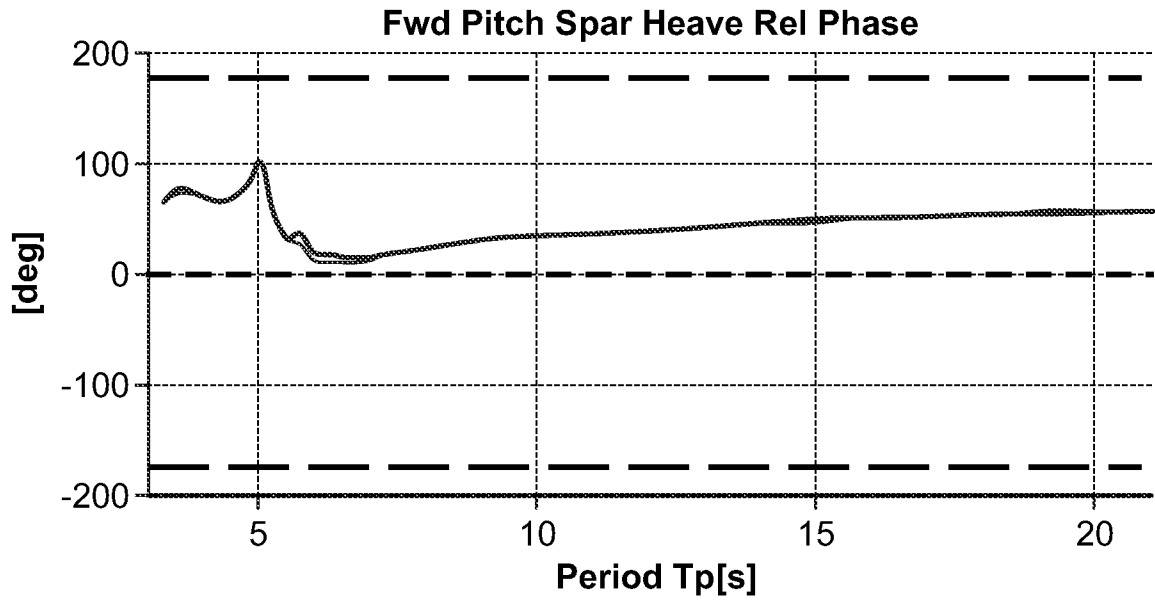
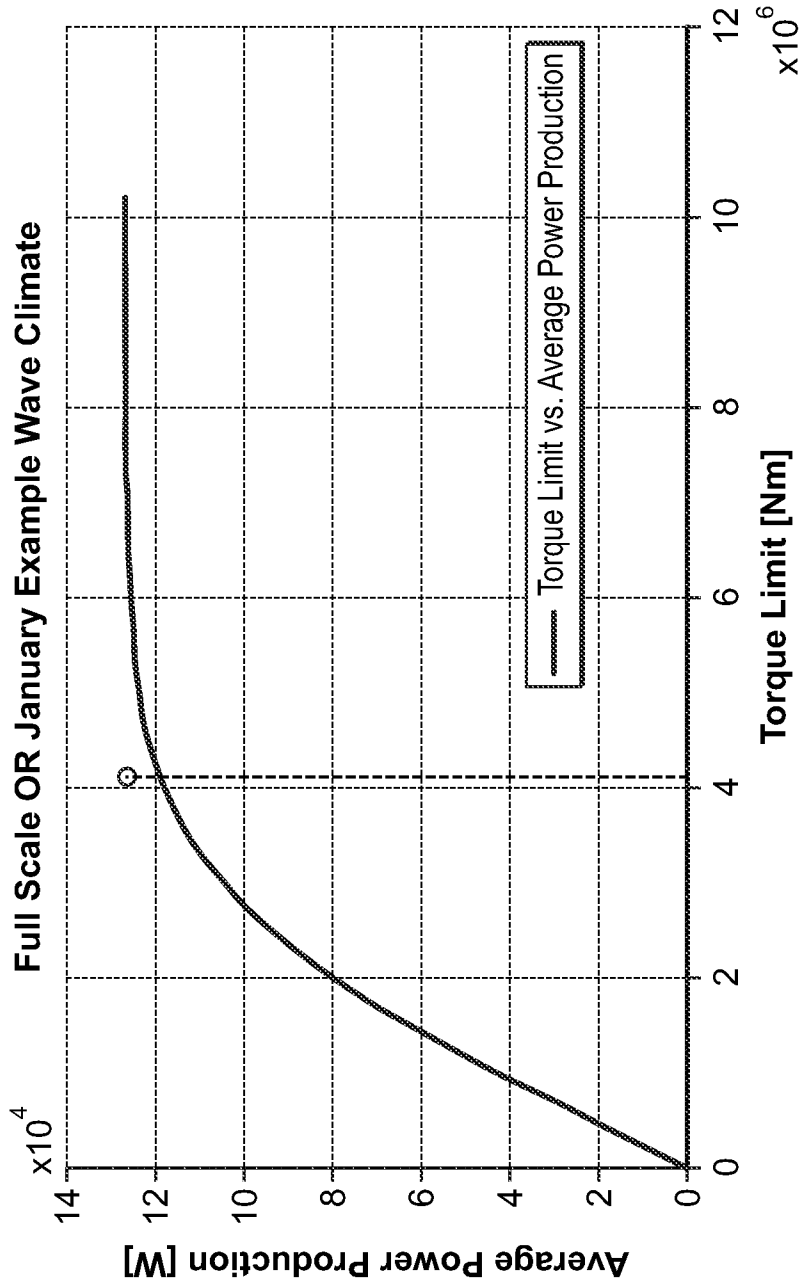
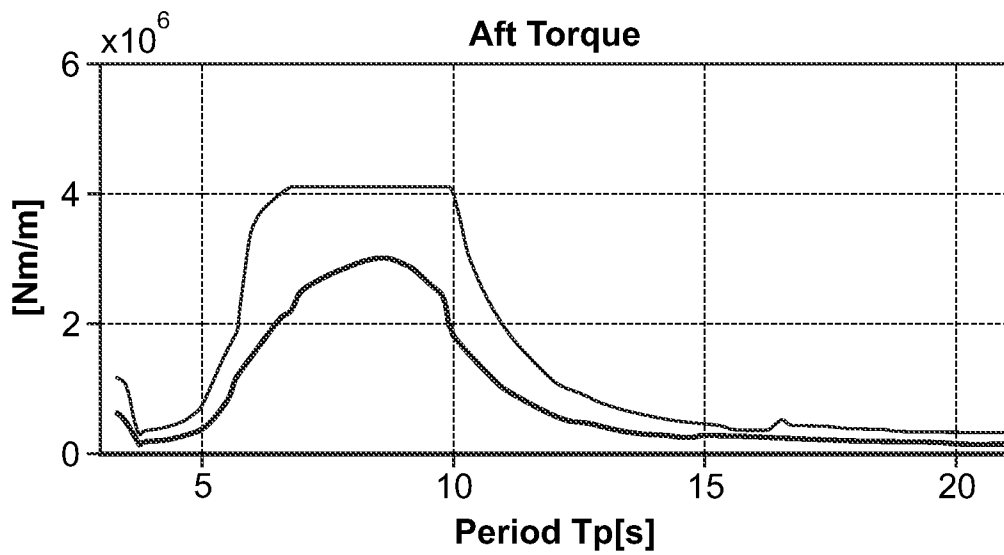
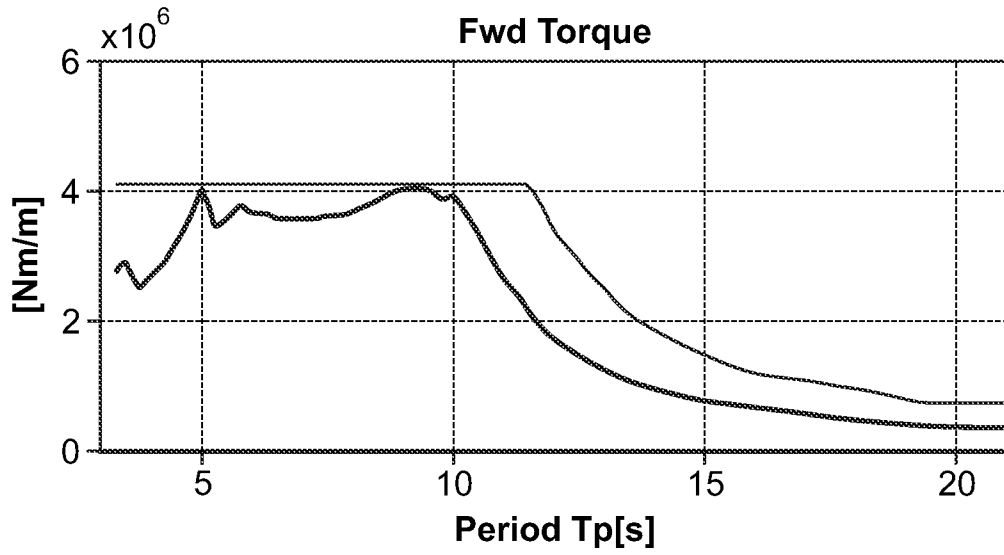


FIG. 15



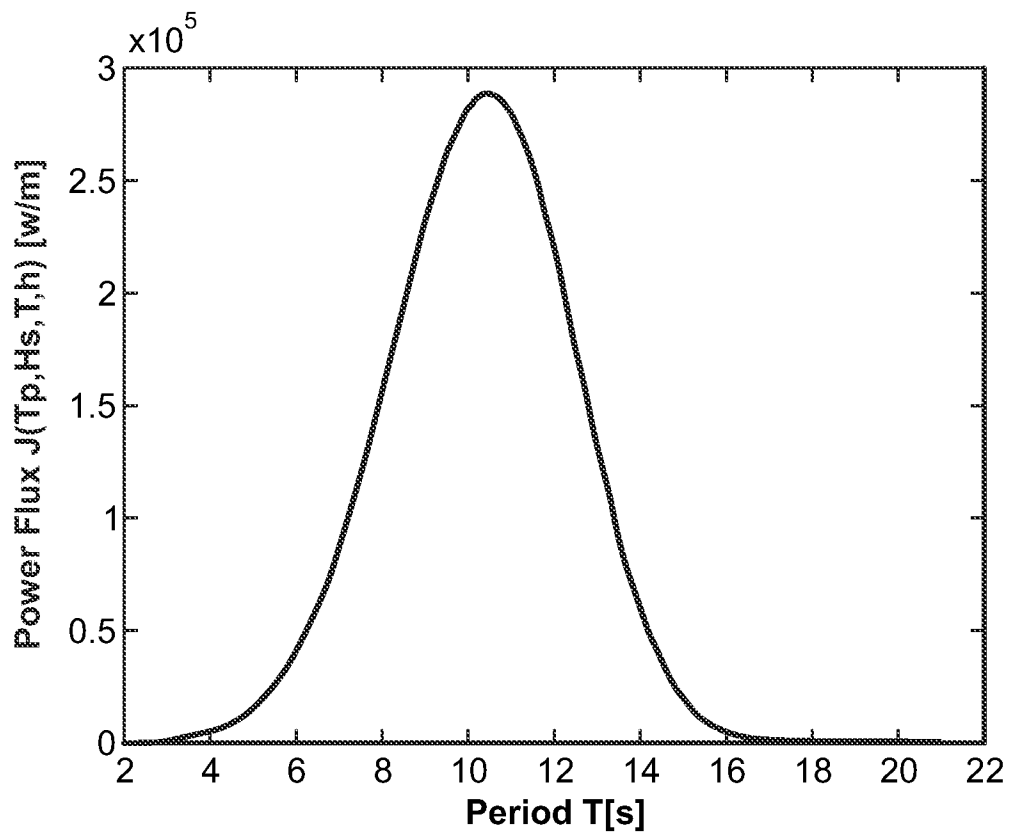
Average power versus imposed torque cap Example

FIG. 16



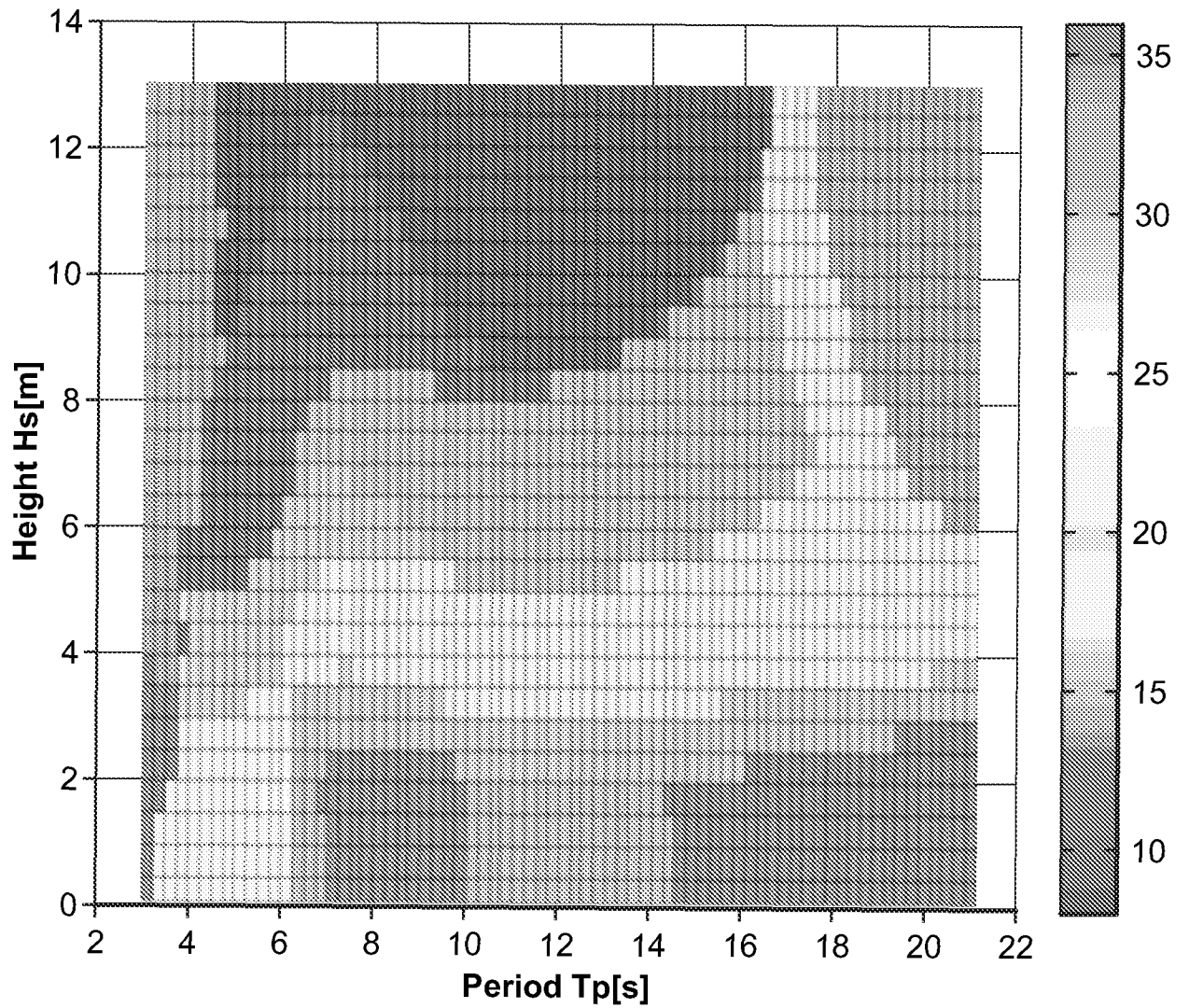
Floats' torque limiting at 4.106 MNm.  $H_s = 2m$ .

FIG. 17



Power per meter at  $T_p = 10$ ses,  $H_s = 2$ m and  $h = 123$ m.

FIG. 18



Best damping cases (1 to 36) for Oregon wave climate (water depth = 123m).

FIG. 19

**Stonewall Banks, OR - OR\_NDBC46050\_S (44.5 °N 124.5 °W)**  
 annual energy = 354 MWh/m, mean power = 40.3 kW/m  
 depth=123m, years; 1996-2008, measured NDBC

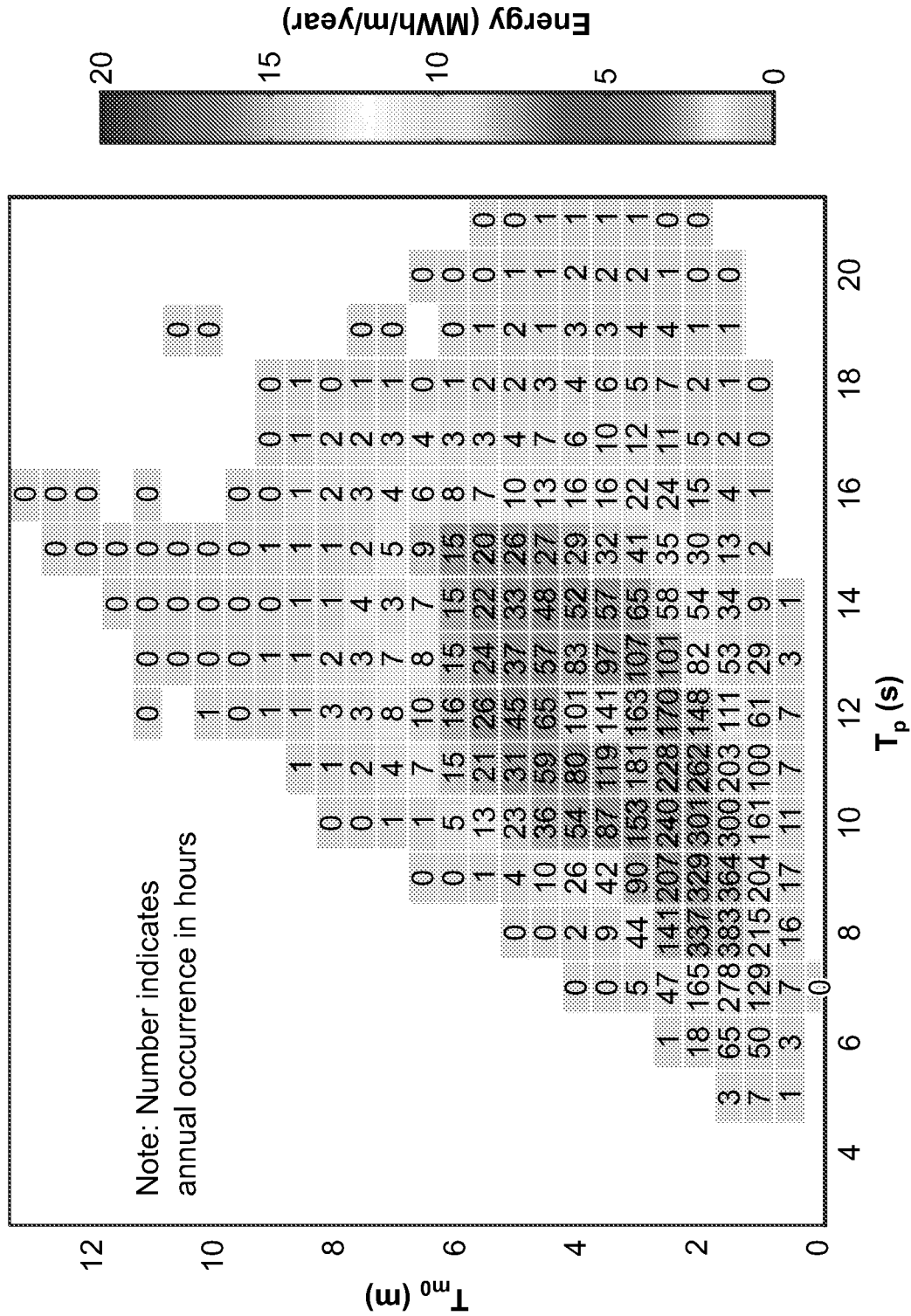


**FIG. 20**

Oregon Occurrence Table. Color scale [MWh/m/year], Number indicates annual occurrence [hours].

	Draft [m]	Total Body Volume [m <sup>3</sup> ]	Submerged Volume [m <sup>3</sup> ]	Mass [kg]	Center of Gravity[m]	Moment of Inertia about CG [kgm <sup>2</sup> ]	Moment of Inertia about Origin [kgm <sup>2</sup> ]
<b>Total System</b>	24.81	1781.4	1592.3	1,566,772.54	x,y,z	Px,Py,Pz	Px,Py,Pz
<b>Spar</b>	24.81	899.5	861.6	876,859.76	0.00 0.00 -15.81	79,973,198 79,640,972 17,816,456	299,080,907 298,748,680 17,816,456
<b>Forward Float</b>	4.81	441.0	365.4	344,956.39	4.9218 0.4125 0.0750	7,440,007 3,692,962 10,237,134	7,521,570 12,063,879 18,661,599
<b>Aft Float</b>	4.81	441.0	365.4	344,956.39	-4.9218 -0.4125 0.0750	7,440,007 3,692,962 10,237,134	7,521,570 12,063,879 18,661,599

CG's are referenced from the origin. Origin at PTO axis and spar body axis.

**FIG. 21**

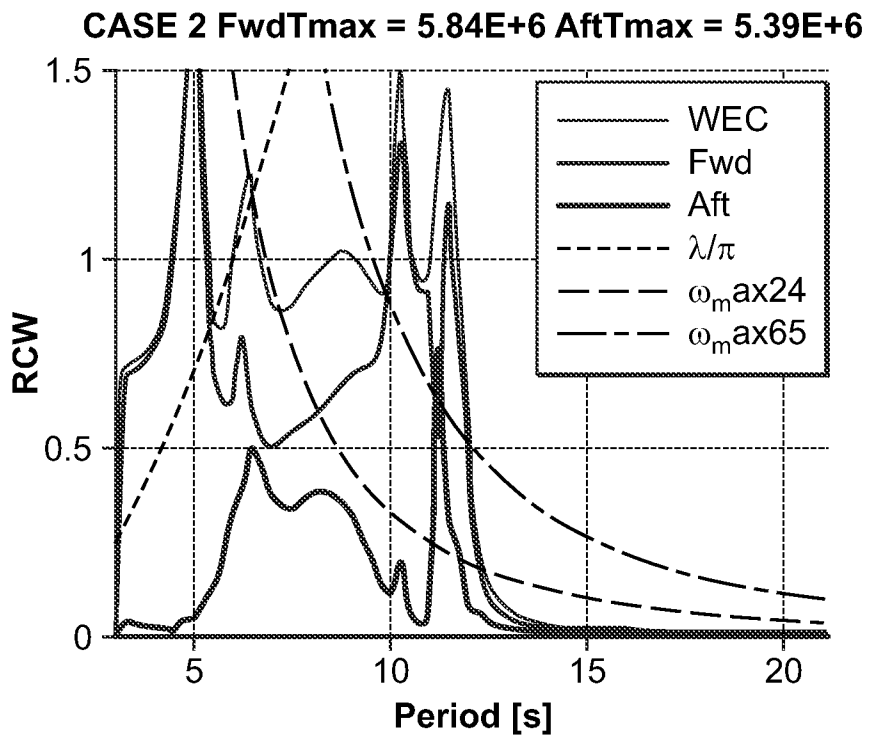
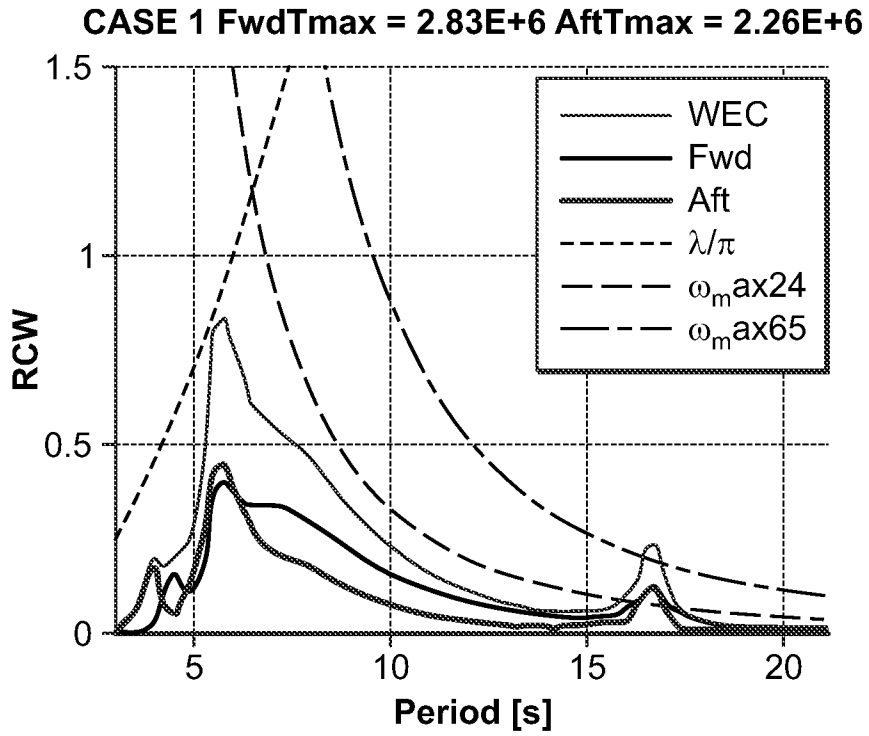


FIG. 22

All ACTIVE RCW Results:

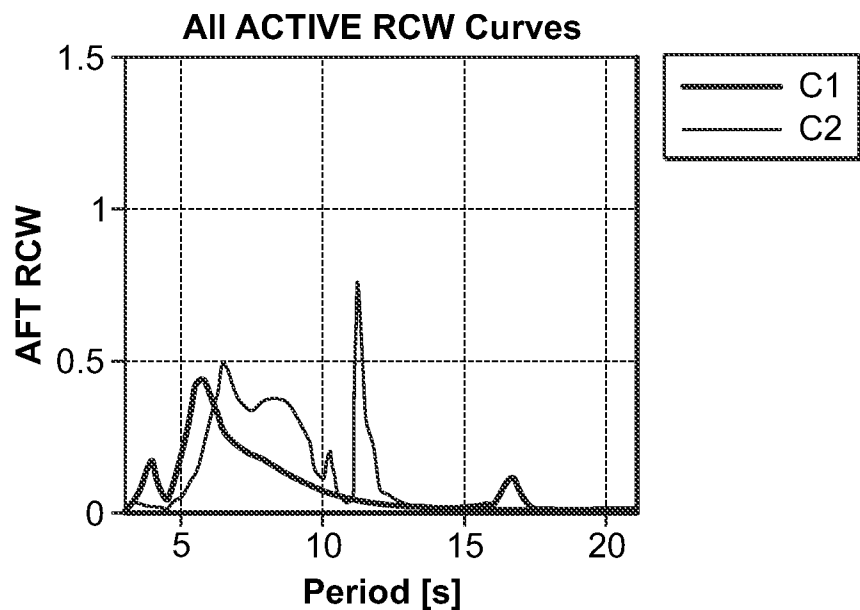
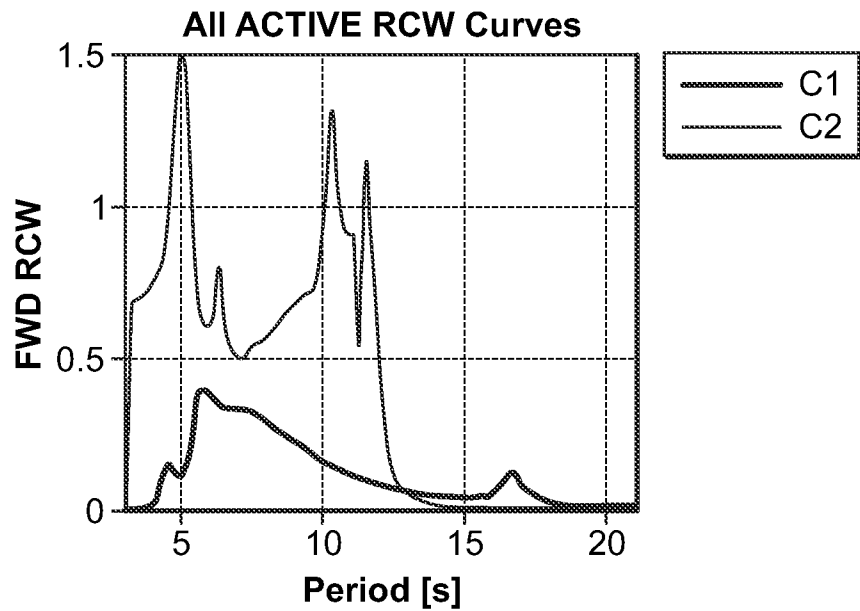
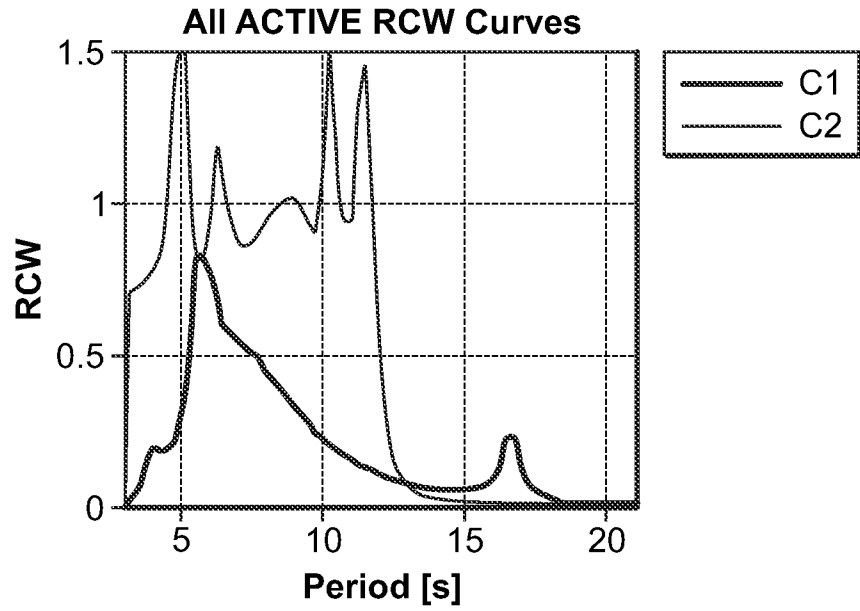


FIG. 23

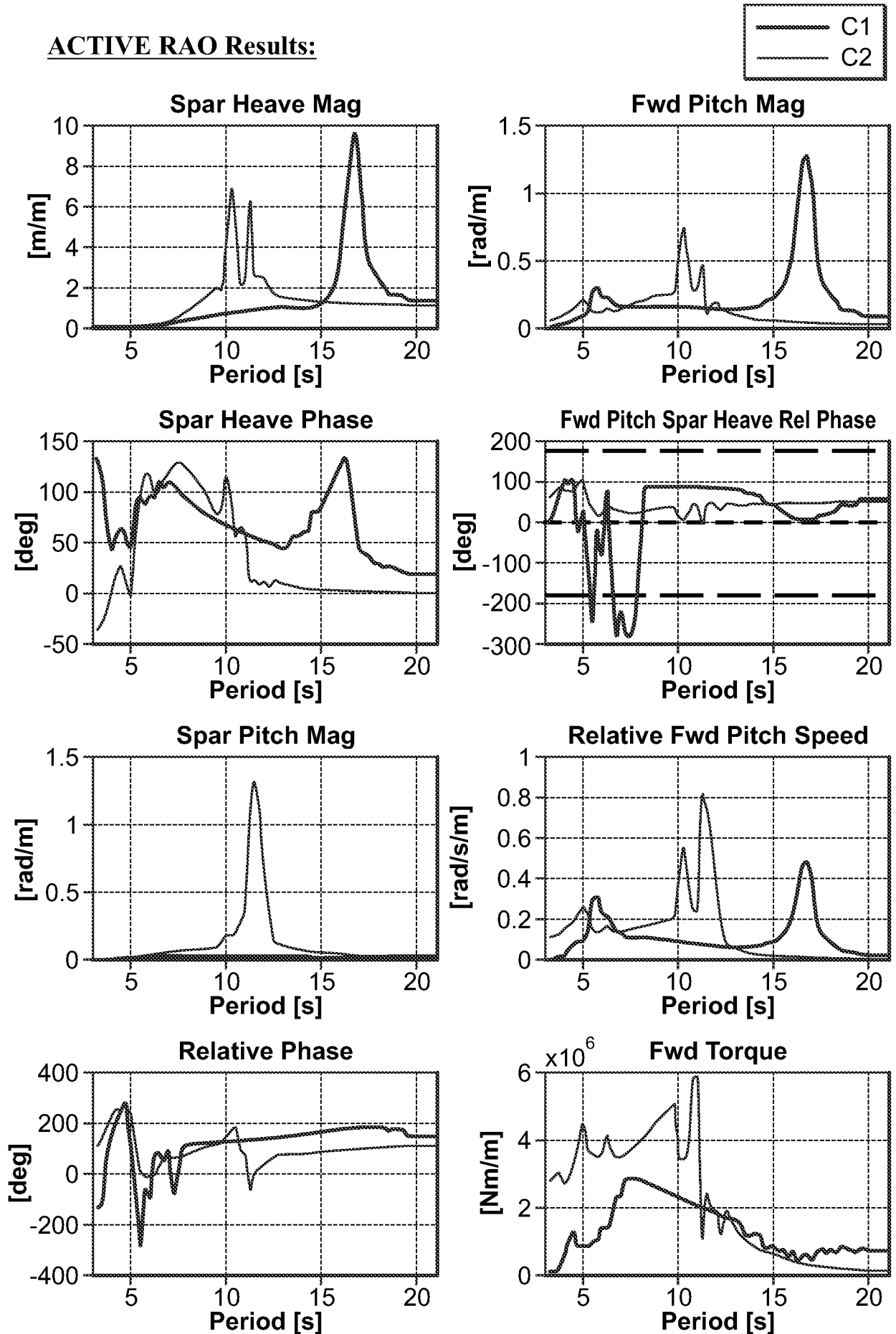


FIG. 24

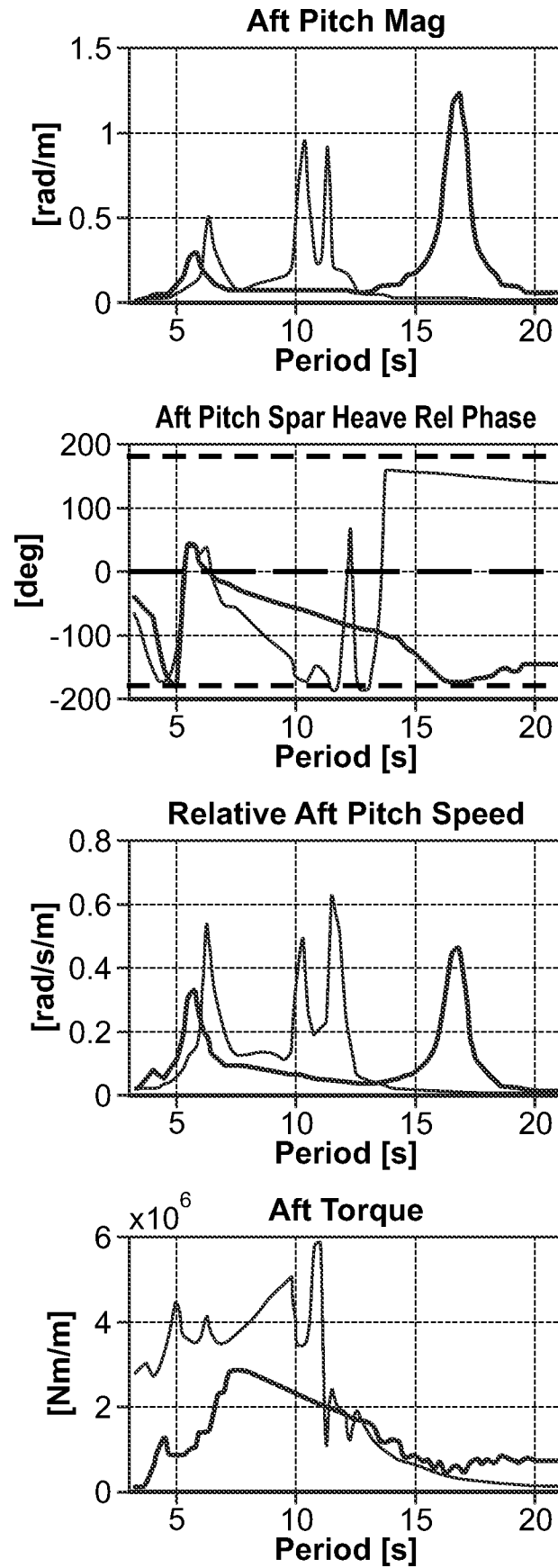


FIG. 24 (Continued)

Damping Conditions:

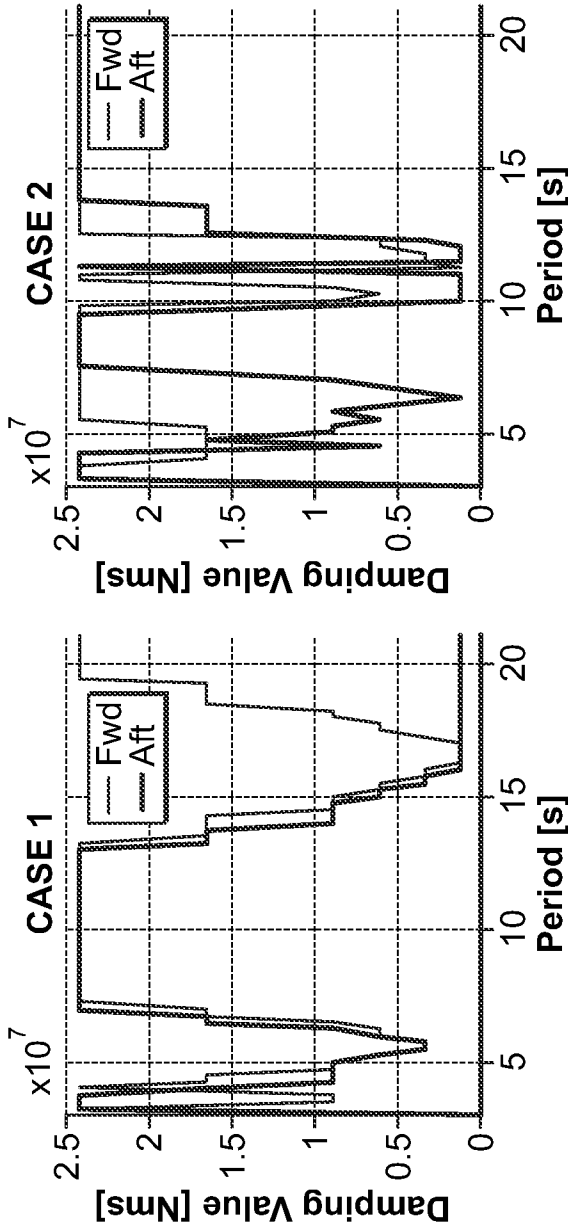


FIG. 25

Energy Spectrum:

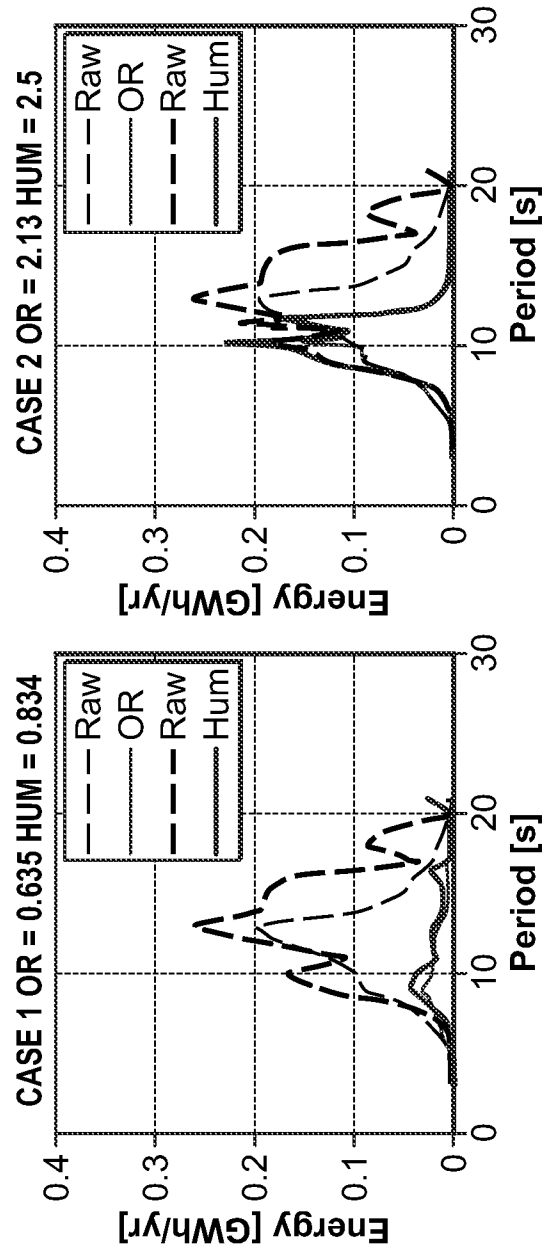


FIG. 26

Energy Climates:

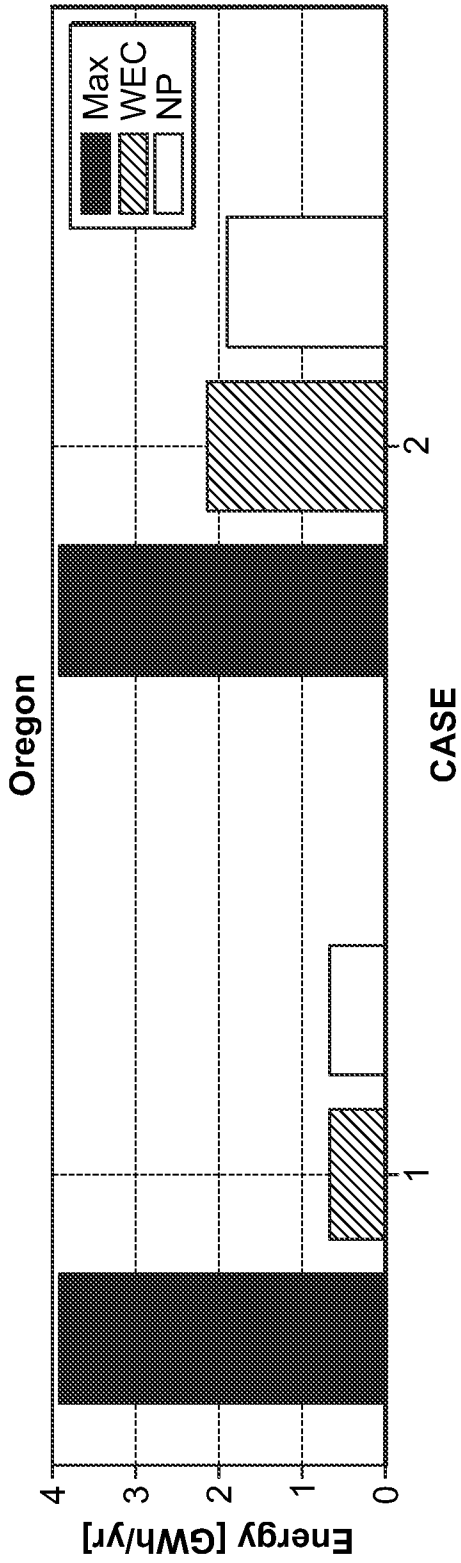


FIG. 27

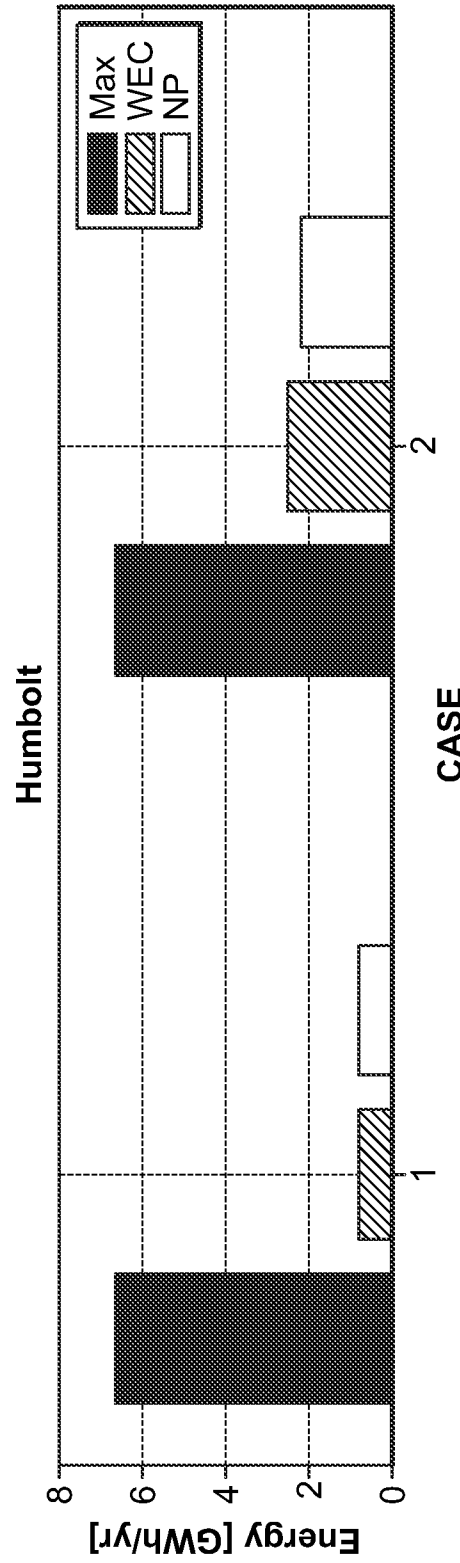


FIG. 28

All Energy Climates:

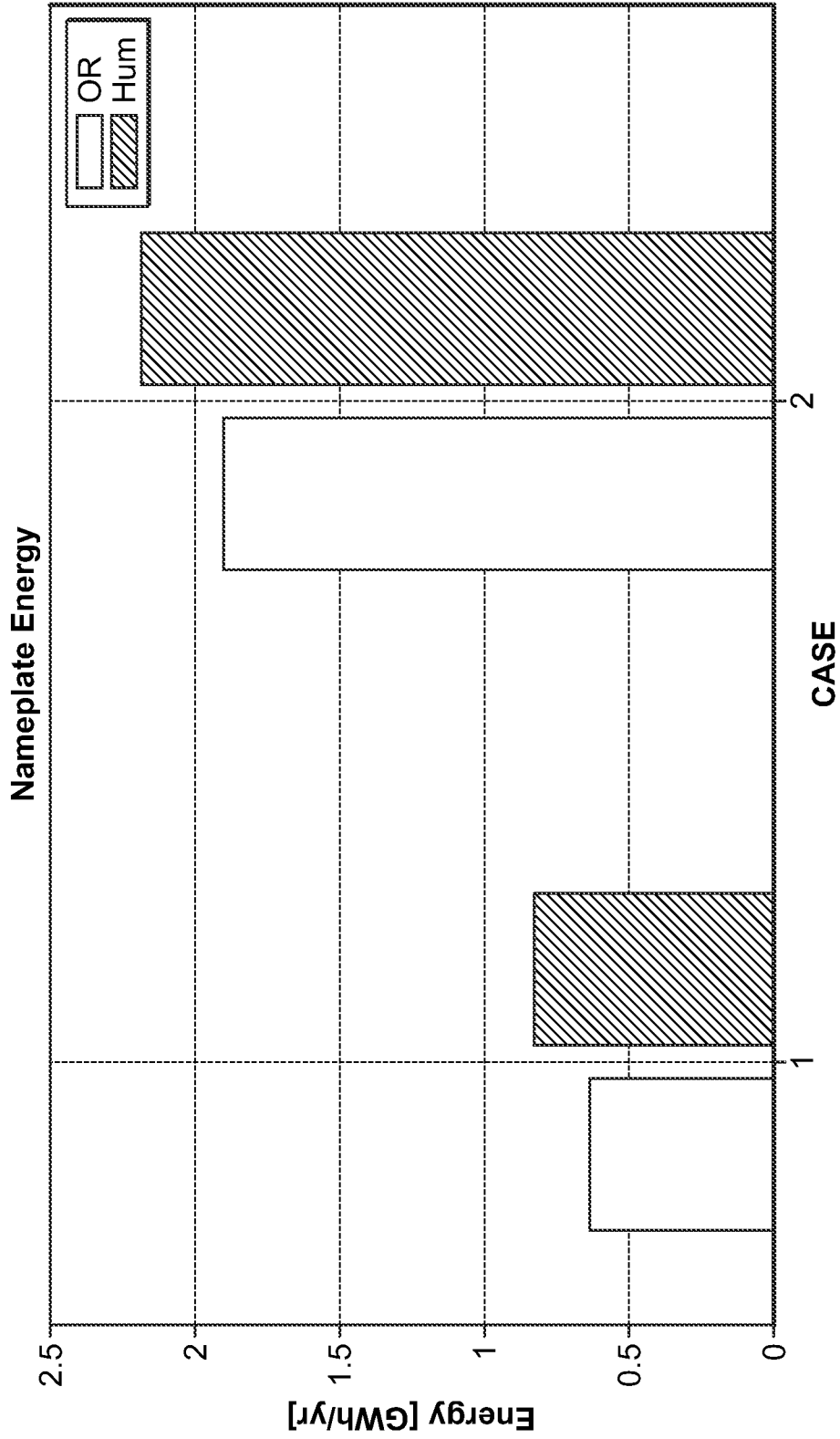
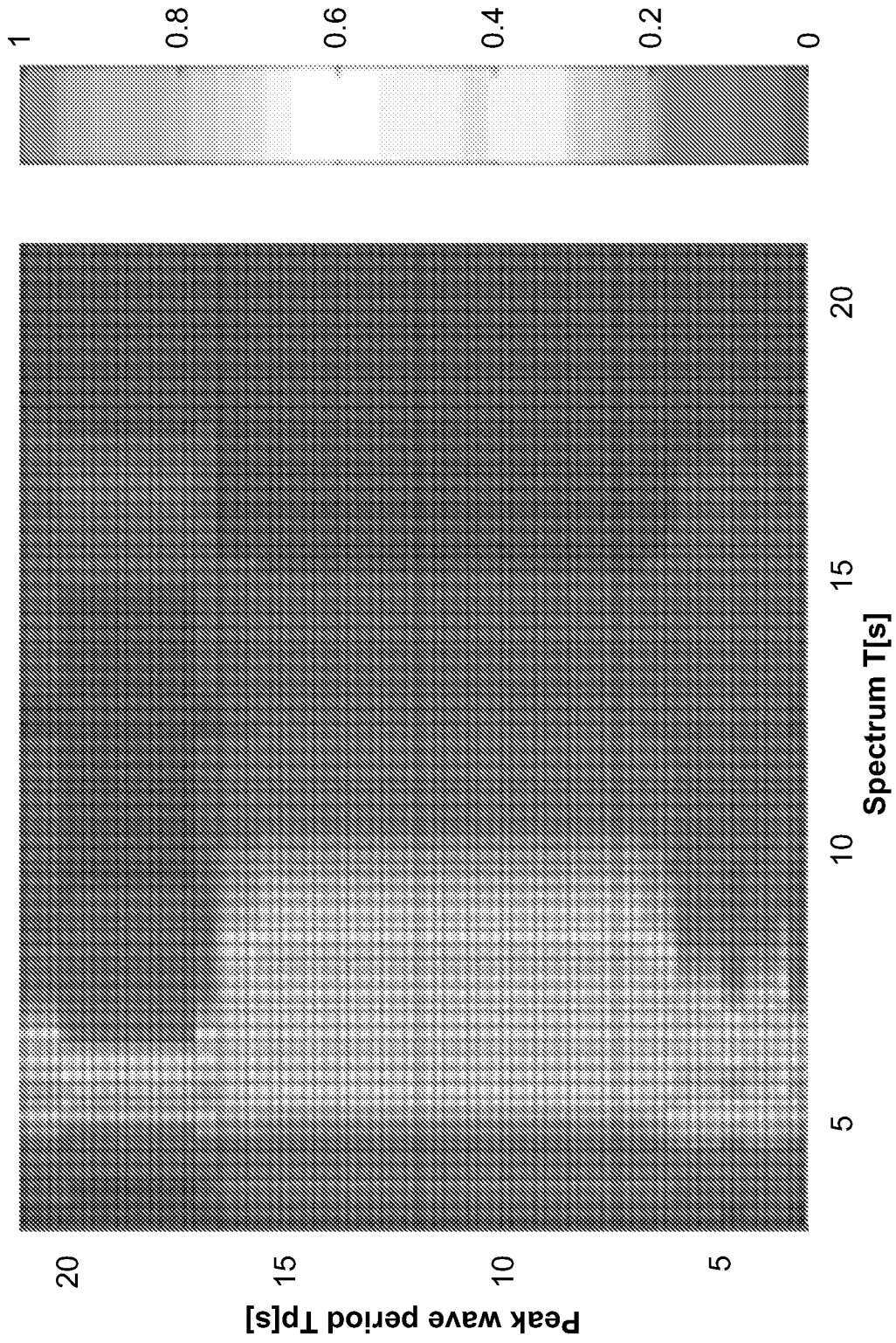


FIG. 29

**ACTIVE RCW from PM Spectrum (top view):**

**CASE 1**



**FIG. 30**

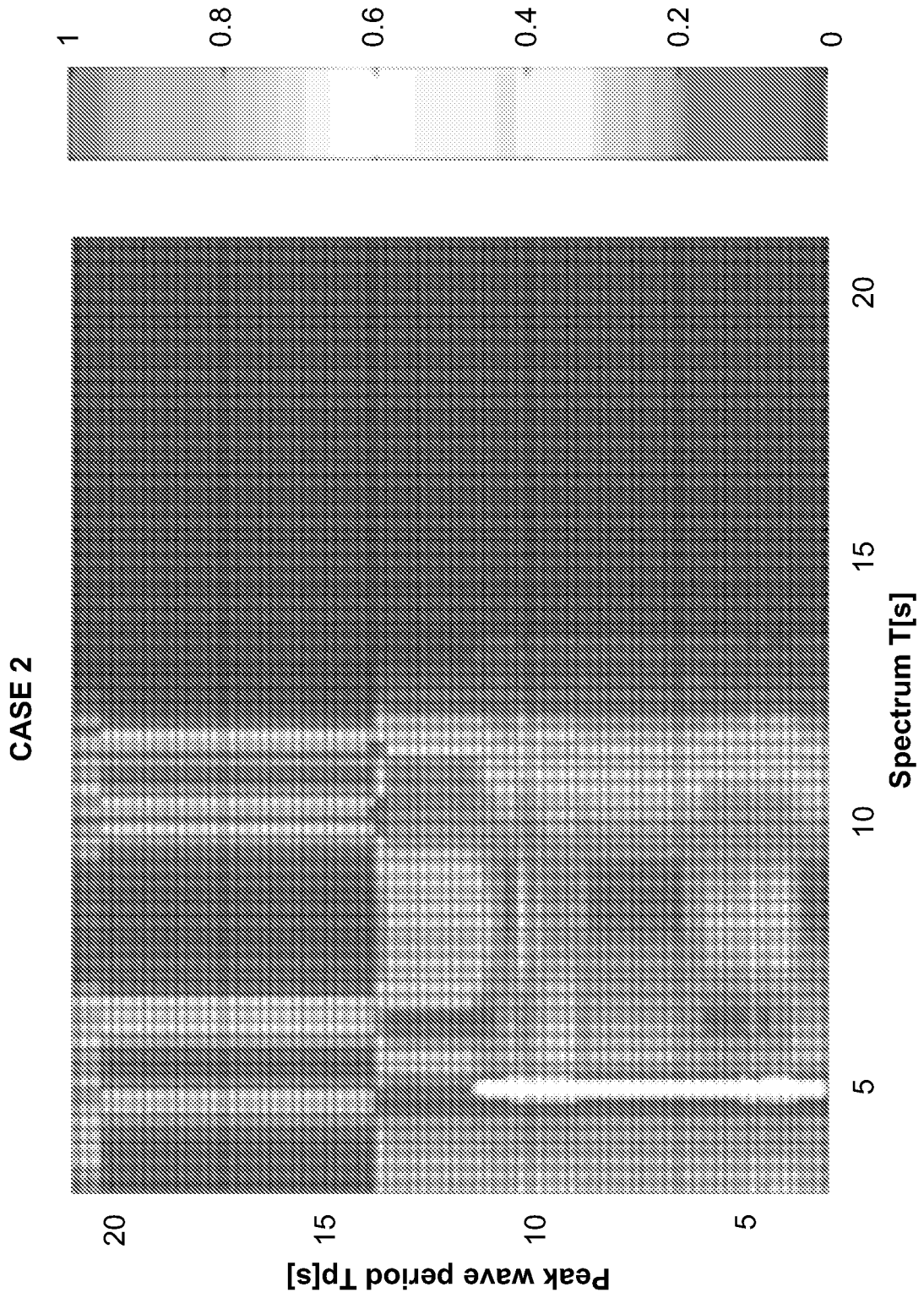


**FIG. 31**

ACTIVE RCW from PM Spectrum (3D view):

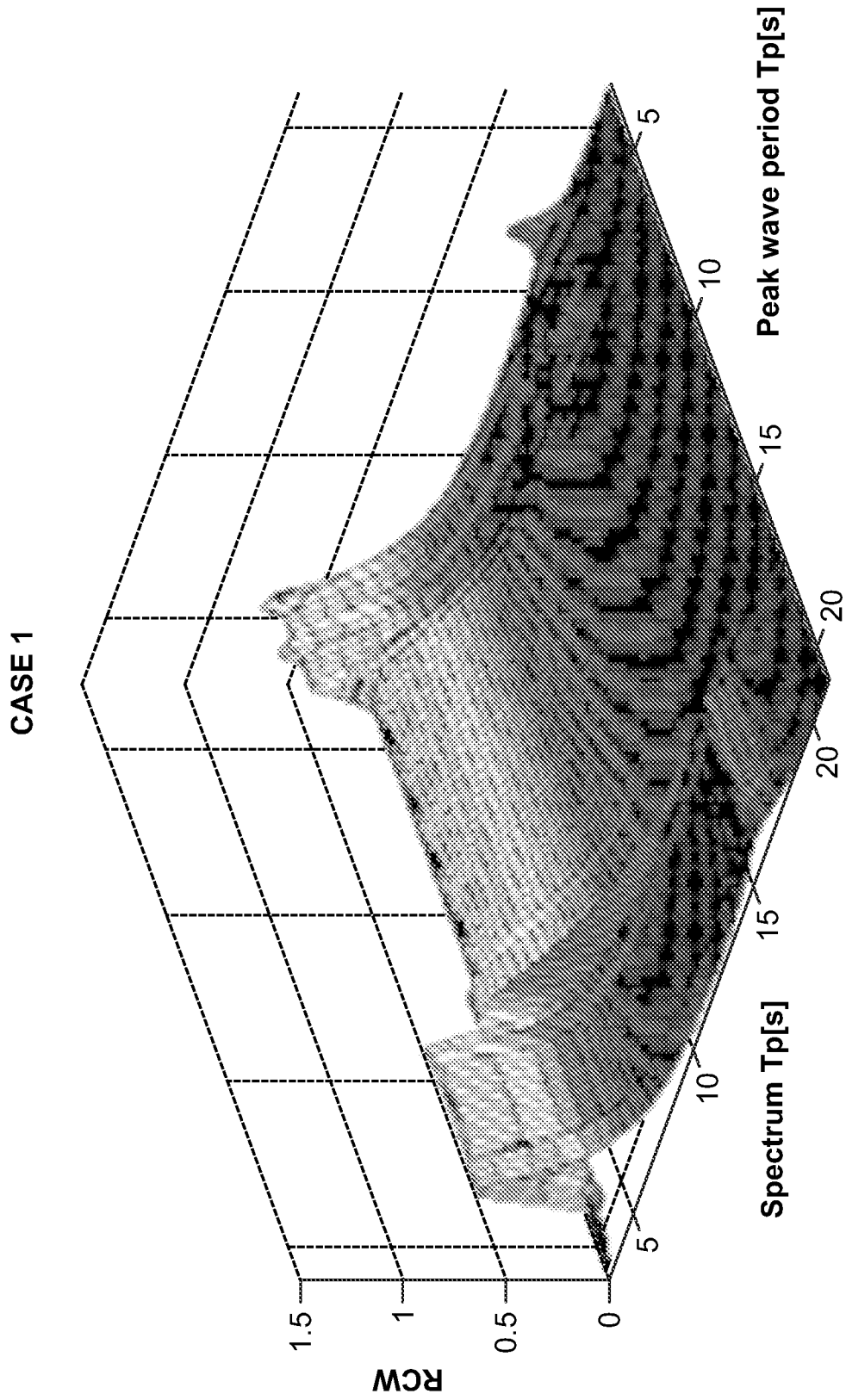
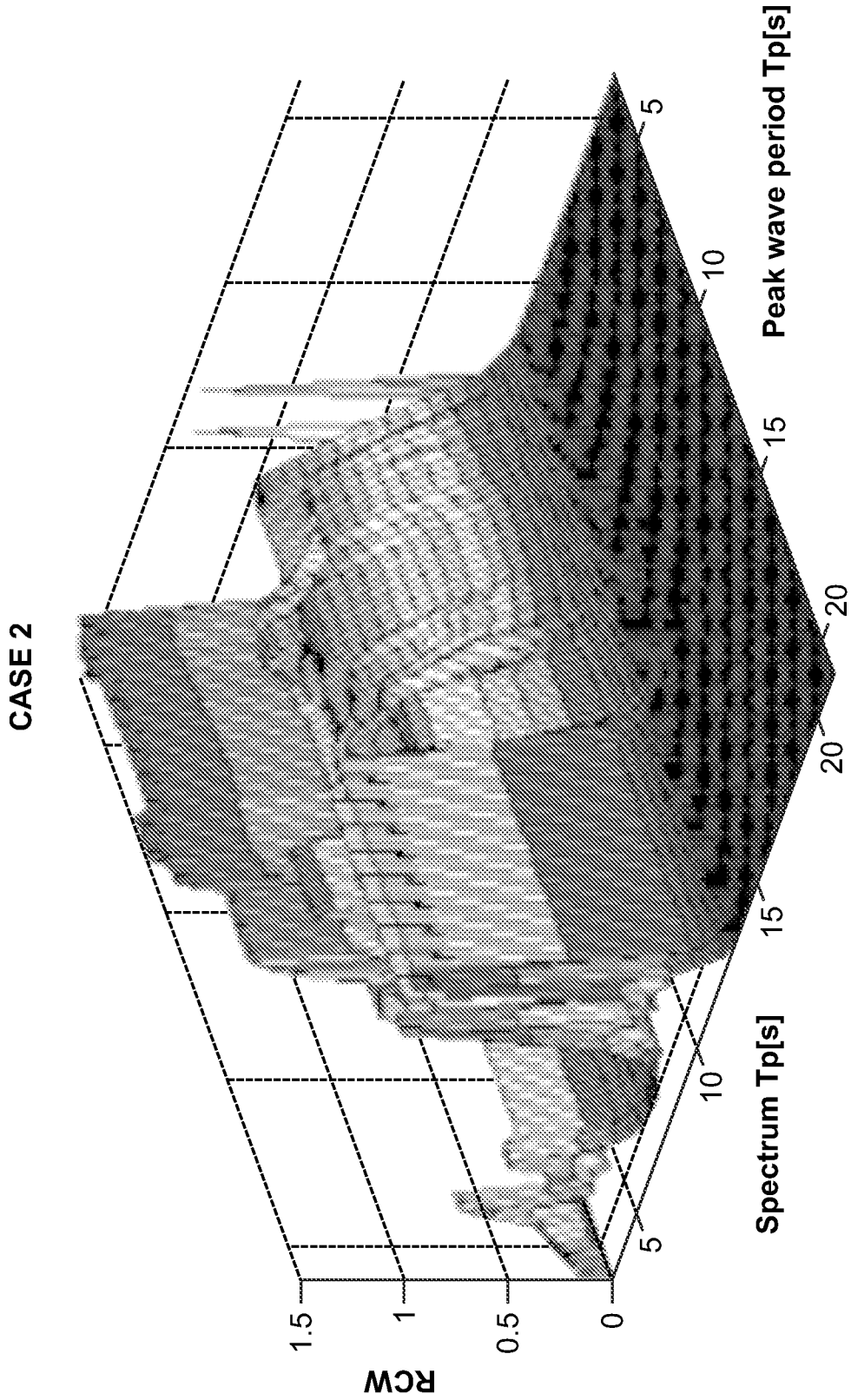


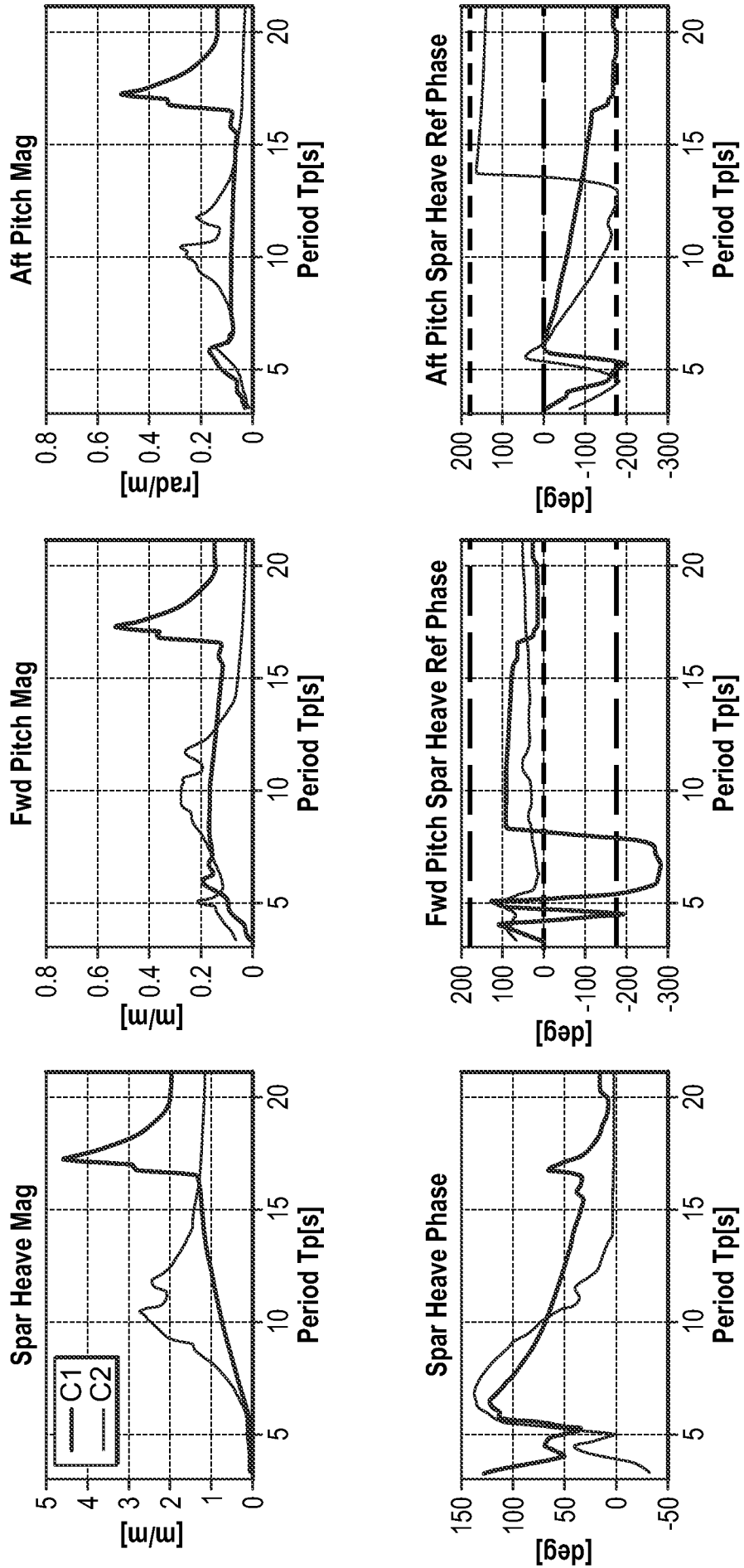
FIG. 32



**FIG. 33**

FIG. 34

ACTIVE RAO from PM Spectrum:



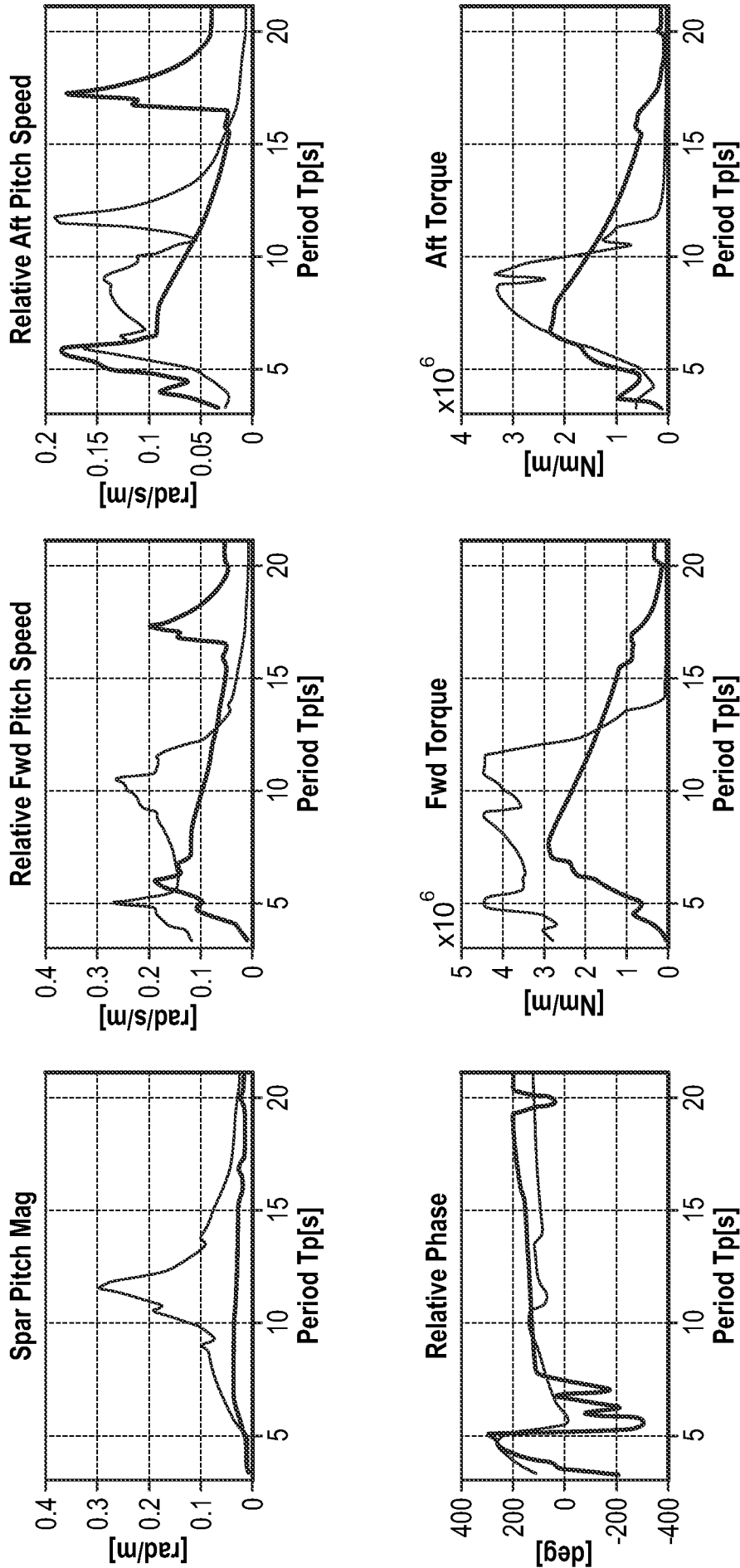


FIG. 34 (continued)

Damping Conditions from PM Spectrum

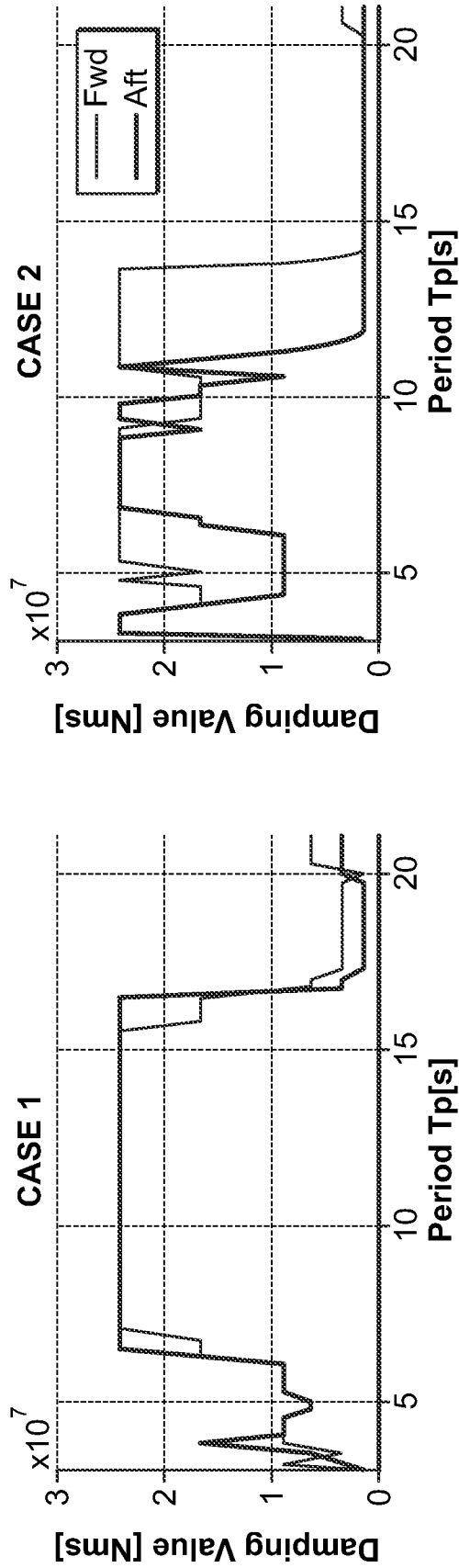


FIG. 35

Damping Selection:

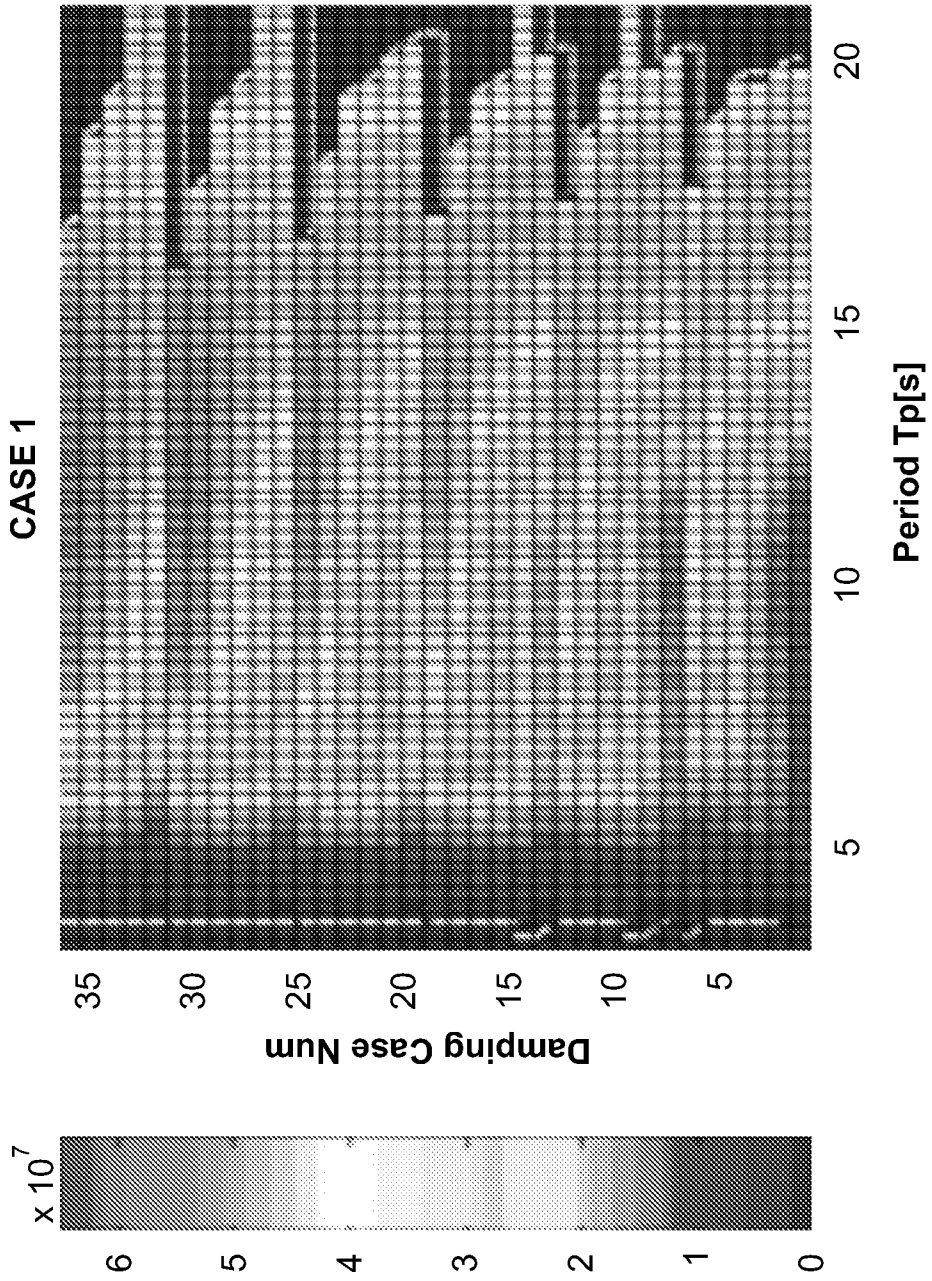
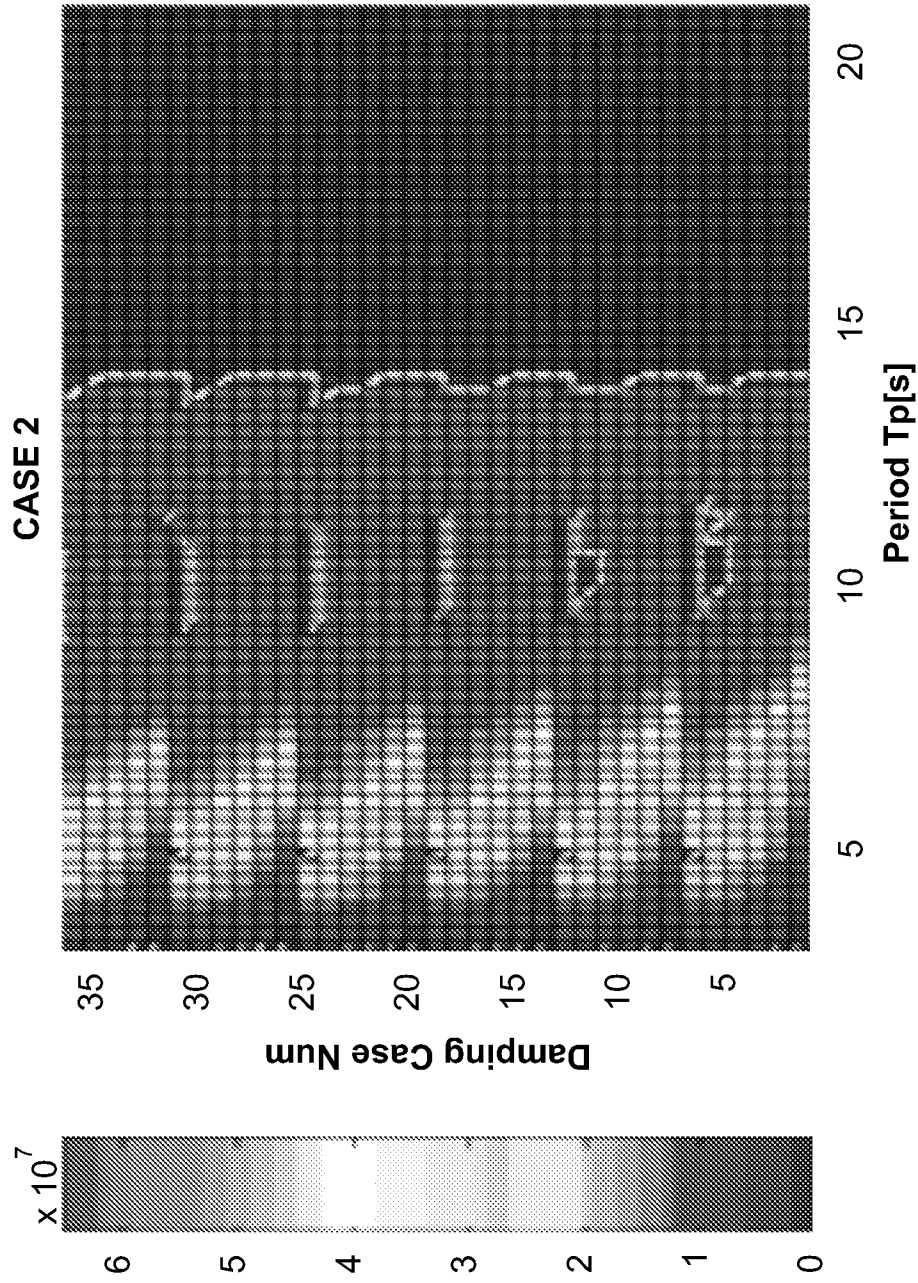


FIG. 36



**FIG. 37**

Energy Spectrum from PM Spectrum:

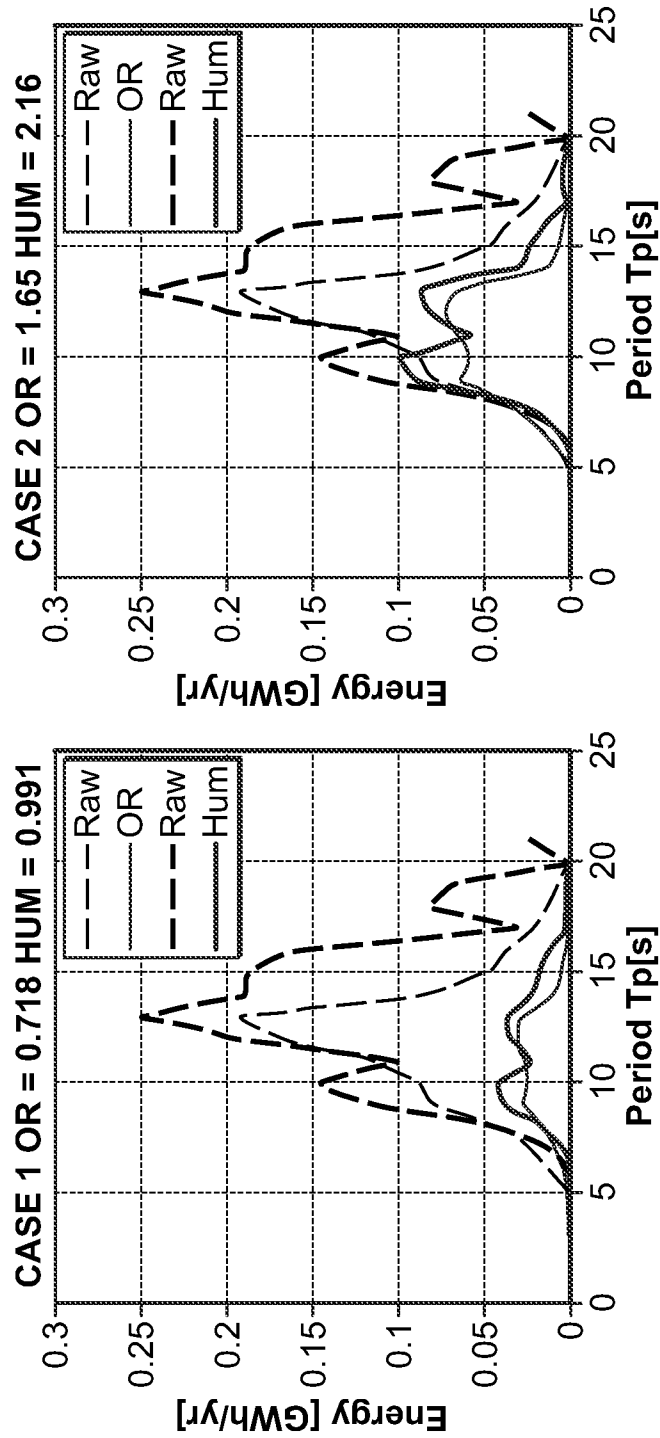


FIG. 38

Energy Climates from PM Spectrum:

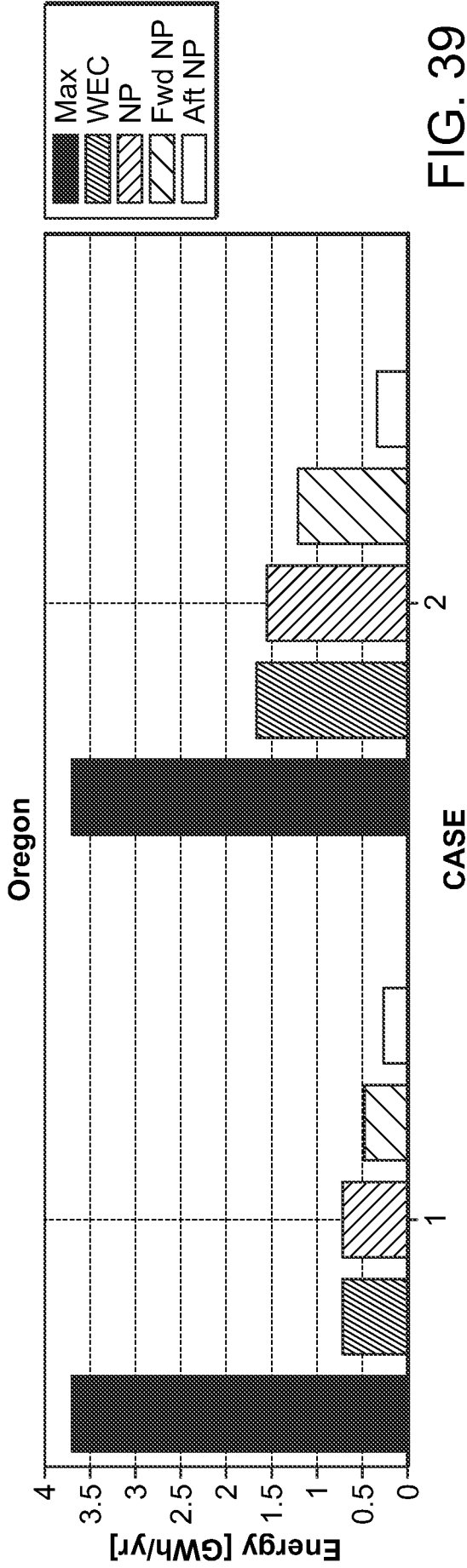


FIG. 39

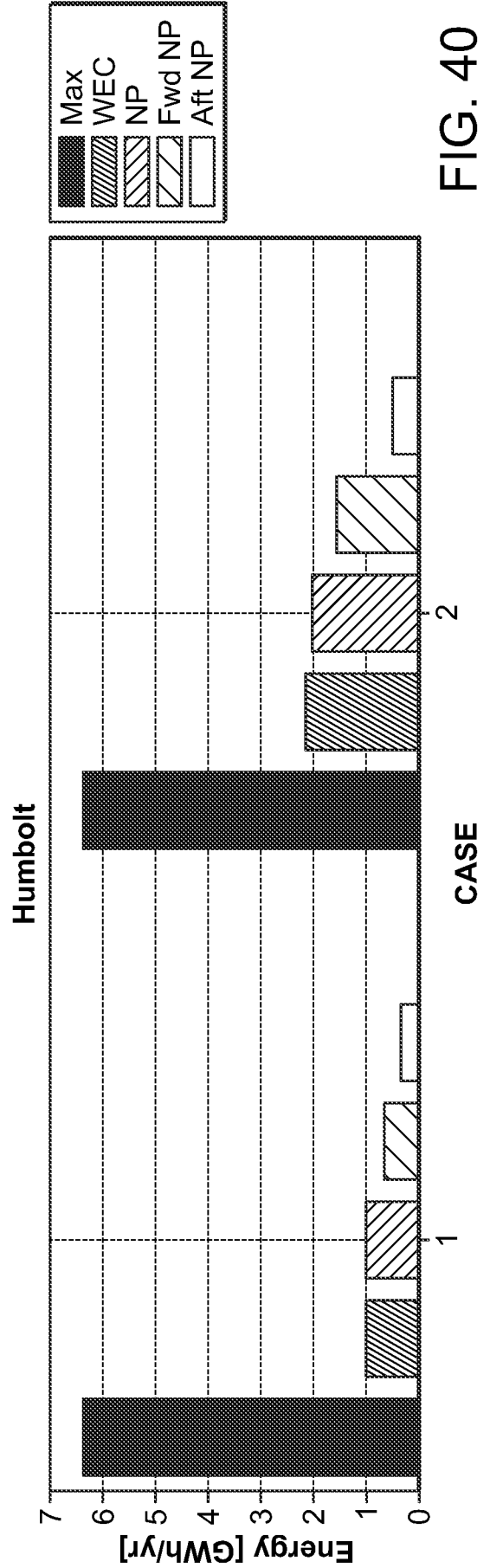


FIG. 40

Active RCW from PM Spectrum:

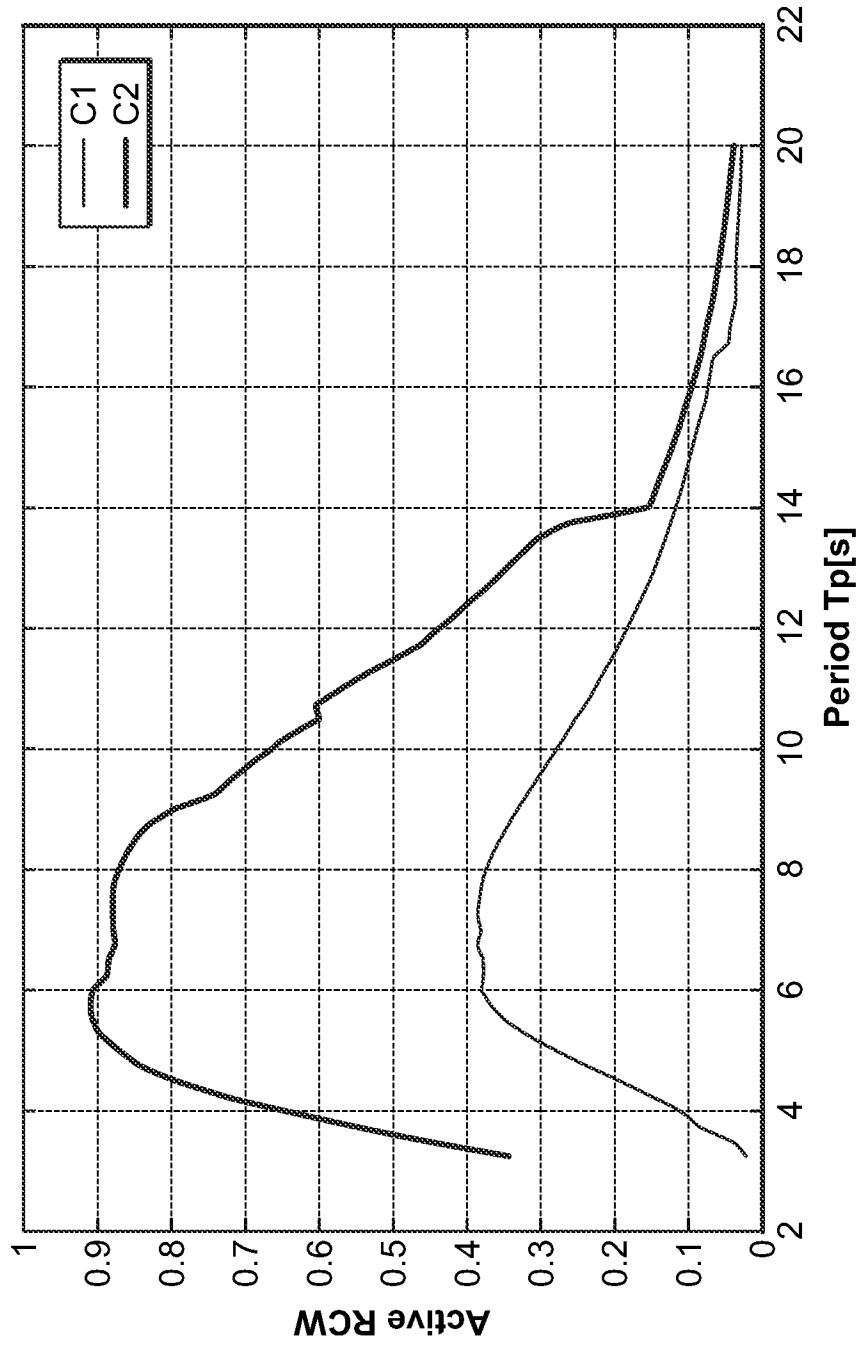


FIG. 41